CHAPTER 8

Motor Systems

To move things is all mankind can do, for such the sole executant is muscle, whether in whispering a syllable or in felling a forest.

Charles Sherrington, 1924

The sensory systems we studied in Chapters 4 and 6 enable animals to know about the world they live in. But sensation is only the first step: to adapt to the world, animals must *act* upon sensory knowledge. For example, animals have evolved the ability to sense the presence of food so they can eat it and obtain energy essential for life. Likewise, animals have evolved the ability to detect danger so that they can fight, hide, or run from it. In the next two chapters, we study the output of the nervous system that makes these active responses to sensation possible.

A key output is the **motor system**, which controls the contraction of skeletal muscles and thereby enables movement, such as reaching for and grasping an object, walking, talking, or maintaining the body's posture. **Figure 8-1** illustrates just one example of how the nervous system exquisitely controls movement, in this case enabling a horse to trot gracefully. We study the motor system in this chapter, with a focus on locomotion control in vertebrates. We will discuss the other two output systems—autonomic and neuroendocrine—at the beginning of Chapter 9.

Movement is produced by coordinated activation of motor neurons driving coordinated contraction of skeletal muscles. In vertebrates, motor neuron cell bodies are located in the spinal cord and brainstem; their axons exit the CNS and innervate specific muscles in the body and head, respectively. Motor neurons are themselves under elaborate control: they receive direct input from proprioceptive

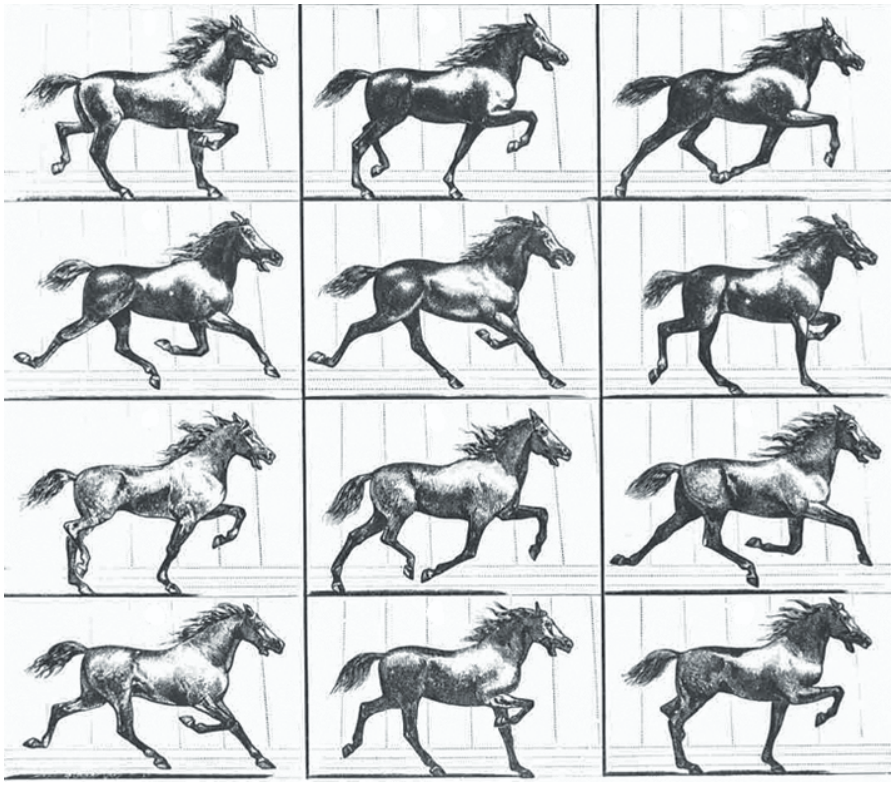

Figure 8-1 The movement of a trotting horse. A complete stride of a trotting horse in 12 frames, engraved after photos by Eadweard Muybridge. These photos (exposure time 1/500 s) showed clearly for the first time that the trotting horse is entirely in the air for part of the stride (frames 4, 5, 9, and 10). (From Muybridge E [1878] *Sci Am* 39[16]:241.)

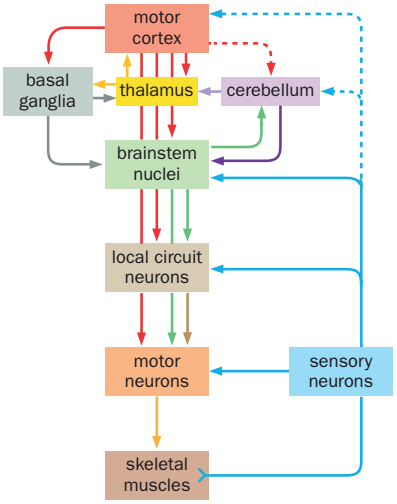

Figure 8-2 Hierarchical organization of movement control. Arrows indicate the direction of information flow. Solid arrows between two regions indicate that at least some connections are direct. Dashed arrows indicate connections through intermediate neurons. While the same neuron can send collaterals that innervate different targets (for example, motor cortex neurons that project to the brainstem and spinal cord often have collaterals in the basal ganglia), separate pathways are drawn for simplicity. The Y-shaped terminal of sensory neurons in the skeletal muscle symbolizes the peripheral endings of proprioceptive somatosensory neurons.

somatosensory neurons, spinal cord premotor neurons, brainstem nuclei specialized in initiating and modulating movement, and (in some species, especially humans) the motor cortex. These descending motor control centers are organized in a hierarchical manner, with the somatosensory system providing feedback signals at multiple levels within this hierarchy. In addition, there are important loops involving the basal ganglia, cerebellum, and thalamus, which add to the sophistication of motor control (**Figure 8-2**). In Chapters 4 and 6, we studied sensory systems by following the direction of information flow, starting with sensory neurons and moving into the brain. We will take the same peripheral-to-central approach in our studies of the motor system, but this time we will address topics in the direction opposite the information flow, starting with muscles and motor neurons and then discussing how layers of upstream neurons and circuits contribute to movement control.

8.1 Muscle contraction is mediated by sliding of actin and myosin filaments and regulated by intracellular Ca^{2+}

Muscle contraction underlies all bodily movement, as reflected in the epigraph. The mechanism of muscle contraction is understood in molecular detail. The muscle cell is an elongated cell composed of thread-like **myofibrils** along its long axis (**Figure 8-3**A). Under electron microscopy, myofibrils are seen to consist of

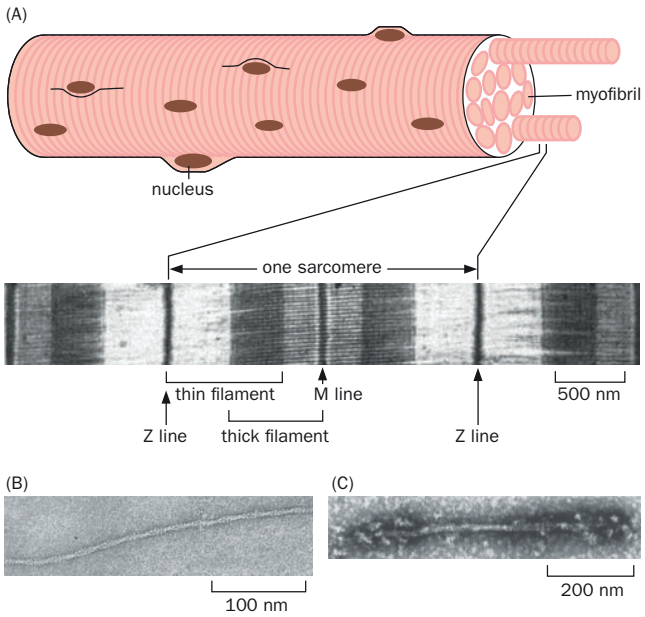

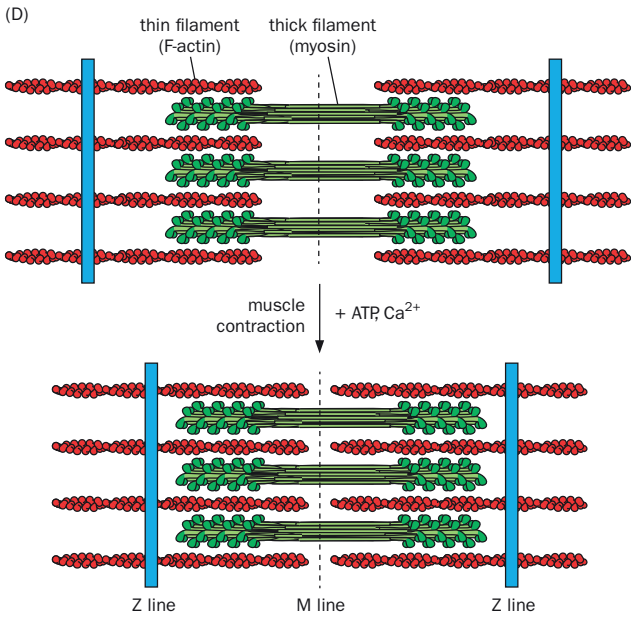

Figure 8-3 The molecular organization of a muscle cell and the sliding filament model of muscle contraction. (A) Top, schematic of a muscle cell, which has multiple nuclei (each muscle cell results from fusion of many myoblasts) and consists of parallel myofibrils. Bottom, as seen under electron microscopy, myofibrils are composed of repeating units called sarcomeres. Each sarcomere is formed by the intersection of thin filaments originating from the Z line with thick filaments originating from the M line. **(B)** A negatively stained electron micrograph shows a microfilament consisting of two F-actin polymer strands; in muscle, F-actin constitutes the major component of the thin filament. **(C)** A negatively stained electron micrograph shows an aggregation of purified myosin, which forms a bare region in the middle and thick protrusions at each end, resembling the organization of thick filaments. **(D)** Illustration of the sliding filament model. The relative movement of thick and thin filaments, caused by myosin motors moving on the actin filaments, underlies muscle contraction. Ca^{2+} is required for myosin–actin interactions. ATP hydrolysis powers this movement. (A–C, micrographs from Huxley HE [1965] *Sci Am* 213(6):18–27. With permission from Springer Nature. See also Huxley AF & Niedergerke R [1954] *Nature* 173:971–973 and Huxley H & Hanson J [1954] *Nature* 173:973–976.)

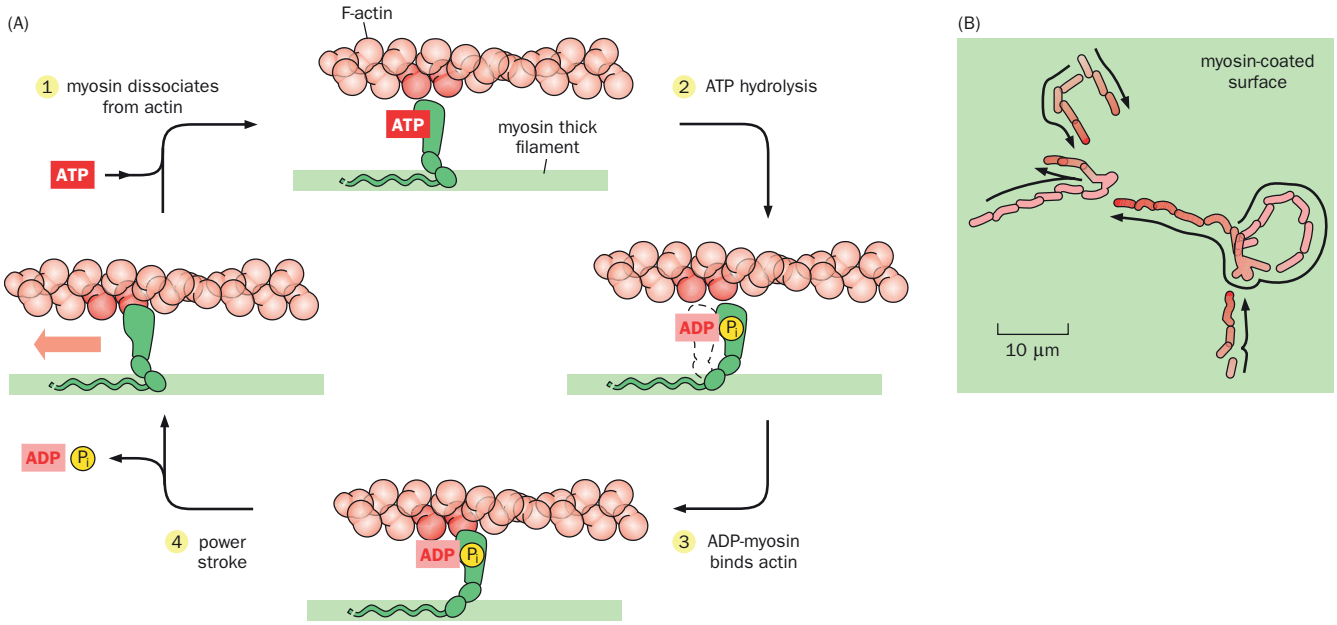

Figure 8-4 ATP hydrolysis powers the movement of myosin and actin filaments relative to each other. (A) The coupled cycles of actin–myosin interaction and ATP hydrolysis. (1) ATP binding to myosin triggers dissociation of myosin and actin. (2) ATP hydrolysis causes a conformational change of the myosin head such that it aligns with the binding surface of the next actin subunit (circles). (3) ADP-myosin binds actin again. (4) ADP and P_i release produces a power stroke—sliding of F-actin against myosin (pink arrow). Note that the myosin head's orientation relative to actin changes with the power stroke. The highlighted actin subunits are shifted one subunit to the right with respect to the actin filament before and after Step 1 to accommodate a new cycle. **(B)** Movement paths of fluorescently labeled actin filaments (rectangles) on a myosin-coated glass slide. Five actin filaments were tracked over the course of 38 s, and their positions are indicated at successive short intervals as they appeared on the video monitor. Arrows indicate the movement direction (darker actin filaments represent later in time). See also Movie 8-2. (A, based on Lymn RW & Taylor EW [1971] *Biochemistry* 10:4617–4624. With permission from the American Chemical Society. B, adapted from Kron SJ & Spudich JA [1986] *Proc Natl Acad Sci U S A* 83:6272–6276.)

repeating units called **sarcomeres**. Each sarcomere is made up of overlapping thick and thin filaments arranged in an orderly fashion. The thin filaments comprise **filamentous actin** (**F-actin**) fibers with several associated proteins (Figure 8-3B). The thick filaments comprise the **myosin** protein (Figure 8-3C). The sliding of thick and thin filaments over each other, mediated by physical interactions between actin and myosin, forms the basis of muscle contraction (Figure 8-3D).

As introduced in Section 2.3, myosin is an F-actin-binding **motor protein**. Myosin has a long tail embedded in the thick filament and a globular head that forms the cross bridge between the thick and thin filaments (Figure 8-3C, D). The head of myosin has an ATPase domain that hydrolyzes ATP. The hydrolysis cycle requires interaction of the myosin head with actin and converts chemical energy from ATP hydrolysis into mechanical force in the form of a **power stroke**, which underlies how myosin and actin move relative to each other (**Figure 8-4**A; **Movie 8-1**). This motility can be visualized in reduced preparations—for example, fluorescently labeled actin filaments were observed to move on a glass slide coated with pure myosin proteins (Figure 8-4B; **Movie 8-2**). Indeed, the movement produced by the interaction of myosin and actin, which was first investigated in the context of muscle contraction, underlies many aspects of cell motility, including cell migration and growth cone guidance (Box 5-2).

Actin/myosin-mediated contraction requires Ca^{2+} (Figure 8-3D), as the F-actin in thin filaments is coated by two proteins called tropomyosin and troponin, which prevent actin from binding to the myosin head under low intracellular Ca^{2+} concentrations. A rise in $[Ca^{2+}]_i$ causes a conformational change in the actin-tropomyosin complex, exposing the actin surface that interacts with myosin.

Ca^{2+} regulation of actin/myosin-mediated contraction forms the link between motor neuron activity and muscle contraction, a process called **excitation-contraction coupling** (**Figure 8-5**). As discussed in Sections 3.1 and 3.12, the arrival

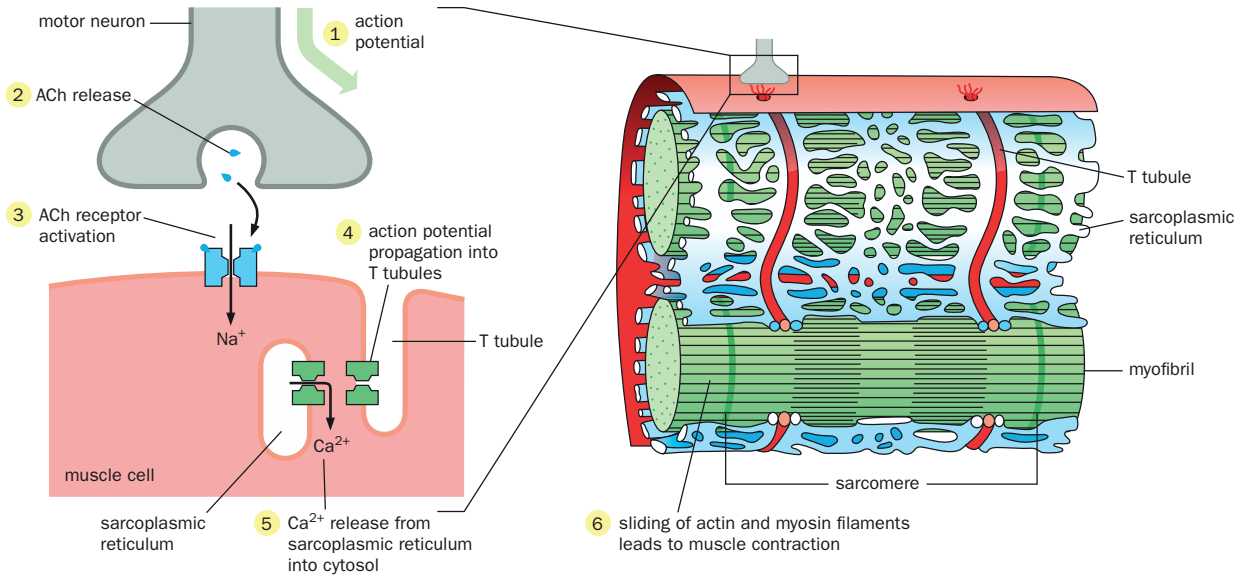

Figure 8-5 Sequence of events from motor neuron excitation to skeletal muscle contraction. The arrival of an action potential at the motor axon terminal (1) triggers acetylcholine (ACh) release (2). ACh binds to the nicotinic ACh receptor on the postsynaptic muscle surface, opening the nicotinic ACh receptor channel and triggering depolarization and action potential production in the muscle cell (3). Action potentials propagate within the muscle cell to T tubules (4) and trigger Ca^{2+} release from nearby sarcoplasmic reticulum into the cytosol (5). Elevated $[Ca^{2+}]_i$ causes muscle contraction (6). (The drawing on the right is adapted from Alberts et al. [2015] Molecular Biology of the Cell, 6th ed. Garland Science.)

of an action potential at the motor axon terminal of the vertebrate skeletal muscle junction causes release of the neurotransmitter acetylcholine (ACh). ACh binds to and opens the nicotinic ACh receptor channel at the neuromuscular junction, which causes depolarization of the muscle cell and production of action potentials within the muscle cell itself. Muscle cell depolarization triggers release of Ca^{2+} from the **sarcoplasmic reticulum**, a special endoplasmic reticulum derivative that extends throughout muscle cells. **Transverse tubules** (**T tubules**), invaginations of the plasma membrane that extend into the muscle cell interior, bring plasma membrane close to the sarcoplasmic reticulum, such that depolarization effectively triggers Ca^{2+} release throughout the large muscle cell. This causes nearly synchronous contraction of all sarcomeres within the same muscle cell, enabling muscles to respond rapidly to commands from motor neurons. Efficient reuptake of Ca^{2+} by the sarcoplasmic reticulum enables muscle cells to respond to repeated commands from motor neurons (**Movie 8-3**).

8.2 Motor units within a motor pool are recruited sequentially from small to large

Each vertebrate skeletal muscle consists of a few hundred to over a million individual muscle cells (also called **muscle fibers**). As discussed in Section 7.13, each muscle fiber is innervated by a single motor neuron in adults. However, each motor neuron innervates multiple muscle fibers, ranging from a few (in an eye muscle) to a few thousand (in a leg muscle). Individual muscle fibers innervated by a single motor neuron are dispersed within a given muscle, such that activation of that motor neuron produces force evenly across the muscle (**Figure 8-6**; Figure 7-30). A motor neuron and the set of muscle fibers it innervates are collectively called a **motor unit**. As neuromuscular junctions are powerful synapses that almost always convert presynaptic action potentials into neurotransmitter release and muscle contraction, the muscle fibers within a motor unit are nearly always activated together. Thus, the motor unit is the *elementary unit of force production* in the motor system.

Motor neurons innervating the same muscle cluster together in the ventral spinal cord or brainstem and constitute a **motor pool** (Figure 8-6); each motor

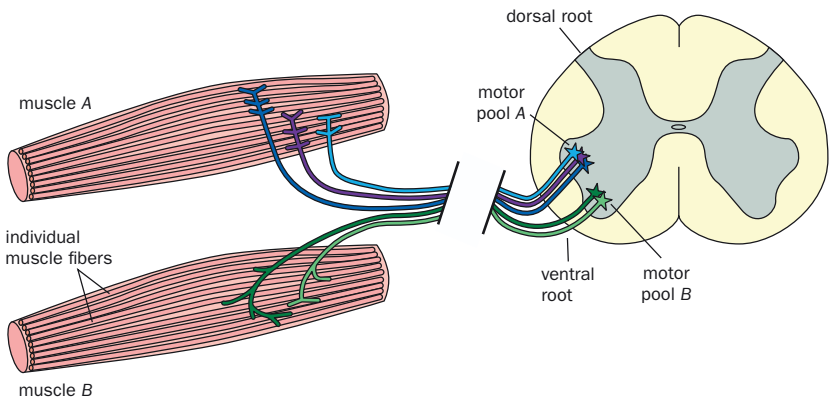

Figure 8-6 Motor pools and motor units. A cluster of motor neurons in the ventral spinal cord constituting a motor pool innervating each muscle. The axons of these motor neurons exit the spinal cord via the ventral root. Two motor pools, *A* and *B*, are shown here. Within each motor pool, individual motor neurons innervate multiple muscle fibers, while each muscle fiber is innervated by a single motor neuron. A motor neuron and the set of muscle fibers it innervates together constitute a motor unit. Motor units vary in size, as is illustrated for the two motor units from motor pool *B*.

pool contains from dozens to thousands of neurons. The **motor unit size**, the number of muscle fibers a motor neuron innervates, varies considerably for neurons within the same motor pool (Figure 7-30). Collectively, motor units within a motor pool follow a **size principle**: neurons that have smaller motor unit sizes usually have smaller axon diameters and cell bodies and are recruited into action before neurons with larger motor unit sizes.

This size principle is illustrated by recordings of motor axon bundles' responses to sensory or electrical stimulation. For example, pressing on the Achilles tendon elicits a stretch reflex that activates the triceps surae muscle in the lower leg (**Figure 8-7**A). The magnitude of triceps surae activation increases as the pressure on the Achilles tendon increases. Researchers recorded from motor axon bundles innervating the triceps surae muscle in response to varying pressure applied to the Achilles tendon. They found that motor axons of smaller units were excited

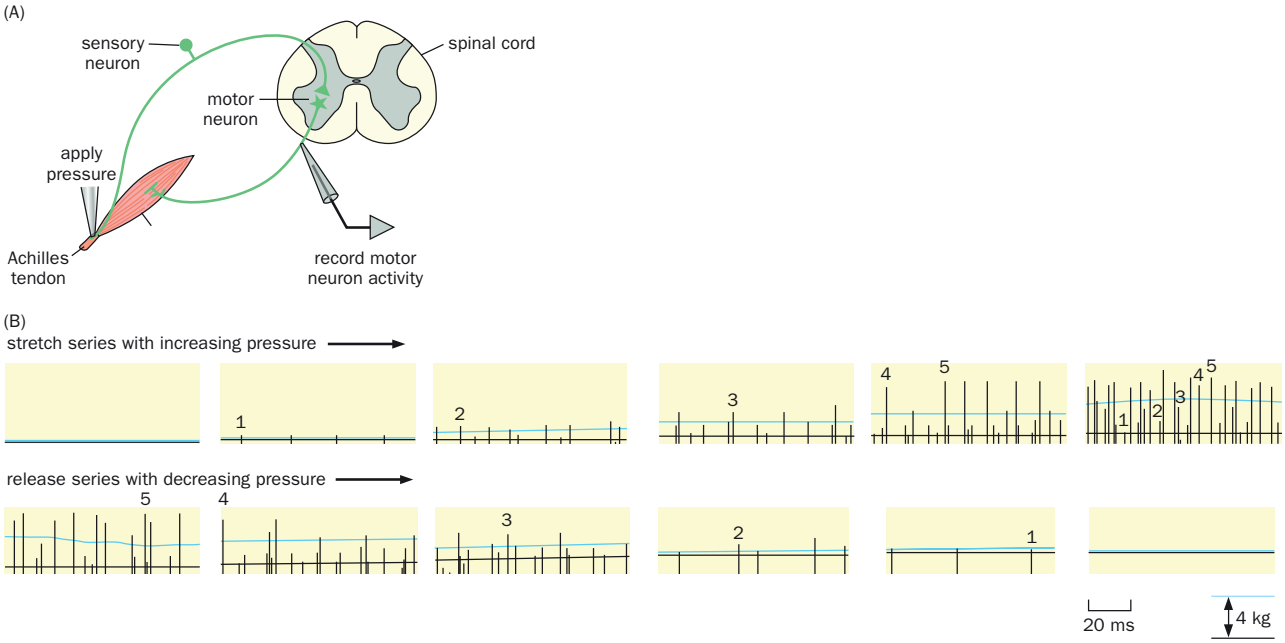

Figure 8-7 Motor units are recruited in order based on their size. **(A)** Schematic of the experimental setup. Nerves innervating all hindlimb muscles except the triceps surae muscle were surgically severed. Pressure was applied to the Achilles tendon via a mechanoelectric transducer to elicit a stretch reflex. Responses of motor neurons innervating the triceps surae muscle were recorded at the ventral root of the spinal cord, where action potentials of different motor neurons can be recorded simultaneously via extracellular recording. The size of the signal (vertical bar in Panel B) correlates with axon diameter and hence with motor unit size. **(B)** Top, as the pressure increases (indicated by the distance between the blue and black horizontal lines, scale at bottom right), sensory neurons' firing rates increase, increasing motor neuron firing through monosynaptic transmission. The smallest motor neuron (1) fires first, followed by motor neurons of increasing sizes (2 through 5). Bottom, as the pressure decreases, the largest motor neuron (5) ceases firing first, followed by motor neurons of descending size (4 through 1). (B, adapted from HennemanE, Somjen G, & Carpernter DO [1965] *J Neurophysiol* 28:560–580.)

by a small amount of pressure and that motor axons corresponding to increasingly larger motor units were recruited sequentially as the pressure increased. In response to gradually reduced pressure on the Achilles, motor axons with the largest units ceased firing first, followed in an orderly manner by axons of decreasing motor unit size (Figure 8-7B). Importantly, this order of motor neuron recruitment does not usually vary—whether the muscles are stimulated by the natural stretch reflex or by direct electrical stimulation—suggesting that it is an intrinsic property of the motor pool.

The size principle of motor units enables incremental control of the magnitude of an individual muscle's contraction in response to excitatory and inhibitory inputs received by its motor pool. Thus, the size principle resembles sensory adaptation and Weber's law we discussed in the context of sensory perception (Section 4.7). When the magnitude of muscle contraction is small, adding or subtracting a small motor unit makes a notable difference; these differences are used to achieve fine motor control. As the magnitude of muscle contraction increases, the size of a motor unit required to make a notable difference in the total contraction strength also becomes larger. The size principle is also important from an energetics perspective. Most movements are small and use only small motor units that consume little energy, whereas large motor units, which exert greater force and consume more energy, are used more rarely.

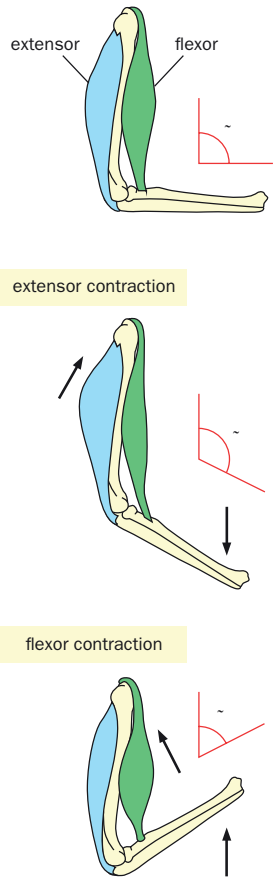

Figure 8-8 Extensor–fexor muscle pair s control the joint angle. Contraction of the extensor muscle increases the joint angle (θ), leading to extension of the joint. Contraction of the flexor muscle decreases the joint angle. The extent and timing of extensor and flexor contraction are coordinated to precisely control the joint angle.

8.3 Motor neurons receive diverse and complex inputs

We now turn to a key question in movement control: how is activation of different muscles coordinated? The principal goal of muscle contraction is to change the joint angle, as in the case of the knee-jerk reflex (Figure 1-19). The angle change is achieved by coordinated action of **extensor** muscles, whose contraction increases the angle (thus extending the joint), and **flexor** muscles, whose contraction decreases the angle (**Figure 8-8**). Extensors and flexors are **antagonistic muscles**, as they perform opposite actions, and they often fire in succession. For example, extension of a joint is initiated by contraction of the extensor and terminated by subsequent contraction of the flexor, so that the joint does not overextend. Complex movements such as the trotting of a horse involve coordinated contraction of many extensor–flexor pairs within each of the four legs, as well as coordination between the legs.

Our discussions so far have indicated that coordination of muscle contraction must be due to coordinated firing of specific motor pools. Therefore, we must learn more about how motor pools are organized and how motor neuron firing is controlled by their inputs. Motor pools that control trunk muscles are located in two bilaterally symmetric medial motor columns running the length of the rostral–caudal axis of the spinal cord, while motor pools that control muscles within each limb form lateral motor columns at the rostral–caudal positions in the spinal cord that innervate each limb (**Figure 8-9**). Within the lateral motor columns, the motor pools that innervate specific limb muscles are located at specific positions. These were originally determined by retrograde tracing (Section 14.18): dye injected into a specific muscle is taken up by axon terminals of motor neurons that innervate that muscle and is transported back to the neuronal cell bodies, resulting in labeling of the corresponding motor pool.

Motor neurons receive very complex sets of inputs. Each motor neuron elaborates a dendritic tree that covers a large area of the spinal cord (Figure 1-15C), enabling it to receive direct input from diverse sources (Figure 8-2). One major source of input comprises excitatory and inhibitory spinal interneurons known as spinal cord **premotor neurons**. The distribution of premotor neurons has been analyzed comprehensively via the retrograde trans-synaptic tracing method (see Section 14.19 for details). **Figure 8-10** shows the distribution of premotor neurons for the motor pool that innervates the quadriceps muscle in the dorsal thigh of the mouse hind limb. Premotor neurons can be ipsilateral or contralateral to the motor pools and are spread across many spinal segments. They consist of multiple transmitter types, including glutamate, GABA, glycine, and ACh. Motor pools

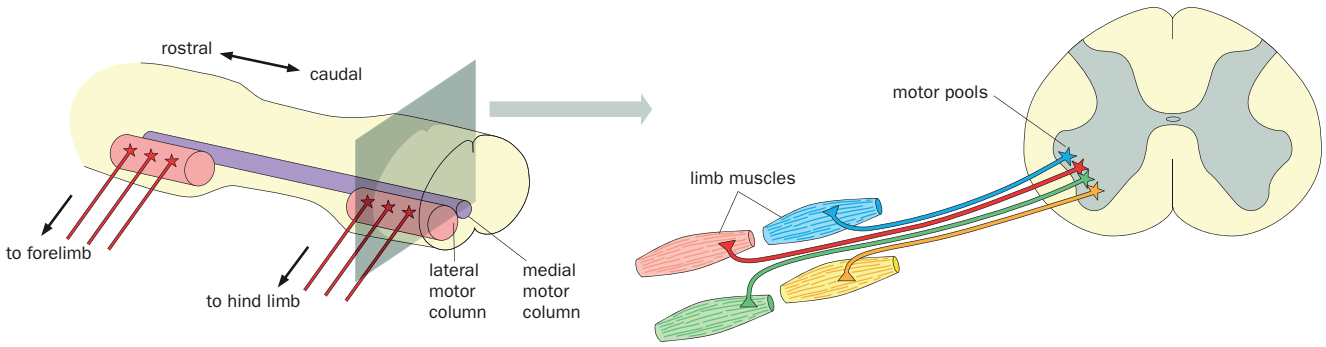

Figure 8-9 Organization of motor columns and motor pools in the spinal cord. Left, motor neurons are organized into motor columns in the ventral spinal cord along the rostral–caudal axis. The medial motor columns regulate trunk muscles, while the lateral motor columns are present at the levels of the spinal cord corresponding to the locations of the limbs and innervate limb muscles. Right, a cross section of the spinal cord at the level of the hind limb. Motor pools that innervate specific muscles (shown as four color-matched pairs) are located in stereotyped positions within the ventral spinal cord. This organization is bilaterally symmetrical (the arrangement is illustrated on only one side).

innervating different muscles receive input from distinct combinations of premotor neurons.

In addition to receiving input from spinal cord premotor neurons, motor neurons also receive monosynaptic input from a small subset of proprioceptive somatosensory neurons, which innervate muscle spindles and form simple reflex arcs (Figure 1-19). These sensory neurons are located in the dorsal root ganglia, and their central axons enter the spinal cord through the **dorsal root** (Figure 6-63), distinct from the **ventral root** where motor axons exit the spinal cord (Figure 8-6). Motor neurons also receive direct descending input from neurons in the brainstem and (in some species) motor cortex, whose axons travel down along distinct pathways in the spinal cord white matter. And, like the motor neurons they regulate, spinal cord premotor neurons themselves receive input from sensory neurons and neurons in the brainstem and motor cortex (Figure 8-2).

The bewildering complexity of spinal cord premotor neurons, along with descending input and sensory feedback, affords exquisite control of motor neuron firing and muscle contraction. It also poses great challenges for researchers trying to discover the principles underlying motor coordination. In the next three sections, we will study one important principle by which rhythmic activation of motor neurons and muscle contraction is achieved.

8.4 Central pattern generators coordinate rhythmic contraction of different muscles during locomotion

Locomotion requires coordinated and rhythmic contraction of many different muscles. For example, in a trotting horse, different leg muscles are activated in a specific sequence to enable each leg to step on the ground, leave the ground, extend forward, and step on the ground again. The four legs are highly coordinated. When the horse slows down to a walk or speeds up to a gallop, the cycle speed for each leg and the synchrony among the legs differ from when the horse is trotting (**Figure 8-11**). How are these motor programs controlled?

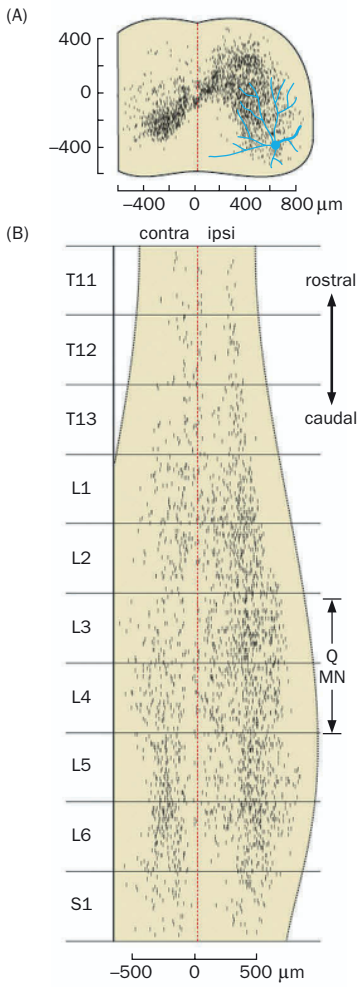

Figure 8-10 Distribution of spinal neurons presynaptic to the motor pool innervating the quadriceps muscle in the mouse right hind limb. Even though the cell bodies of quadriceps motor pools (Q MN) are restricted to the two spinal segments indicated, their presynaptic premotor neurons (dots) are widely distributed, as seen from **(A)** a transverse projection of the spinal cord and **(B)** a longitudinal projection covering thoracic (T), lumbar (L), and sacral (S) segments. A drawing of the dendritic arbor of a typical Q motor neuron (cyan) is superimposed in Panel A. The dotted red line represents the midline of the spinal cord. (Adapted from Stepien AE, Tripodi M, & Arber S [2010] *Neuron* 68:456–472. With permission from Elsevier Inc. Motor neuron drawing courtesy of Silvia Arber.)

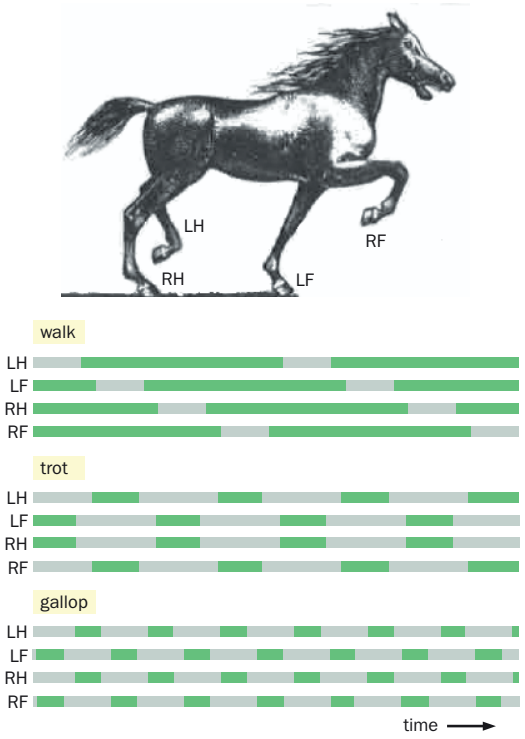

Figure 8-11 Stepping patterns of a horse during walking, trotting, and galloping. From left to right, each horizontal bar represents for a single leg the time off (gray segments) and on (green segments) the ground. During trotting, the left hind leg (LH) and right foreleg (RF) move in sync, as do the right hind leg (RH) and left foreleg (LF). During galloping, the two forelegs are in sync, as are the two hind legs. (Adapted from Pearson K [1976] *Sci Am* 235[6]:72–86. With permission from Springer Nature.)

Recall the knee-jerk reflex discussed in Section 1.9: proprioceptive sensory neurons transduce mechanical stimulation in the spindle of the extensor muscle to activate extensor motor neurons through monosynaptic excitation and simultaneously inhibit flexor motor neurons through an intermediate spinal cord inhibitory neuron (Figure 1-19). An early hypothesis of "chained reflexes" proposed that rhythmic movement such as walking was due to sequential activation of spinal reflexes. Specifically, movement of a leg caused by contraction of a muscle would produce feedback from proprioceptive sensory neurons, which would activate a second motor pool and its corresponding muscle through the spinal cord reflex circuits. This would trigger activation of a second set of sensory neurons that in turn would activate a third motor pool and muscle, and so on, until the original muscle would be activated again, completing the chained reflex cycle.

The chained reflex hypothesis predicts that (1) the spinal cord with intact sensory feedback should be sufficient for rhythmic activation of muscles and (2) when sensory feedback is blocked, rhythmic activation of muscles should cease. The organization of the spinal cord made testing these predictions possible, since transecting dorsal roots would block sensory feedback to motor neurons without affecting connections between motor neurons and muscles, which leave the spinal cord through ventral roots (Figure 8-6). An experiment to test these hypotheses was performed a century ago. In this experiment, all hind limb muscles of an anesthetized cat were surgically inactivated except for one extensor–flexor pair in the lower leg, so that contraction of the extensor and flexor could be measured accurately. A spinal transection rostral to the segments controlling the hind limb was found to induce a transient rhythmic and alternate contraction of the remaining extensor and flexor that mimicked normal walking. (Spinal transection induces massive glutamate release, which mimics excitatory input from the brainstem, as we will discuss later.) Importantly, when dorsal roots were transected to eliminate sensory feedback, the pattern and frequency of alternate contraction of the extensor and flexor induced by spinal transection persisted (**Figure 8-12**A). These results supported prediction (1), as rhythmic contraction of the extensor and flexor could indeed be supported by an isolated spinal cord disconnected from descending control. (As we will learn later, the rhythmic activity must be *initiated* by the brain-

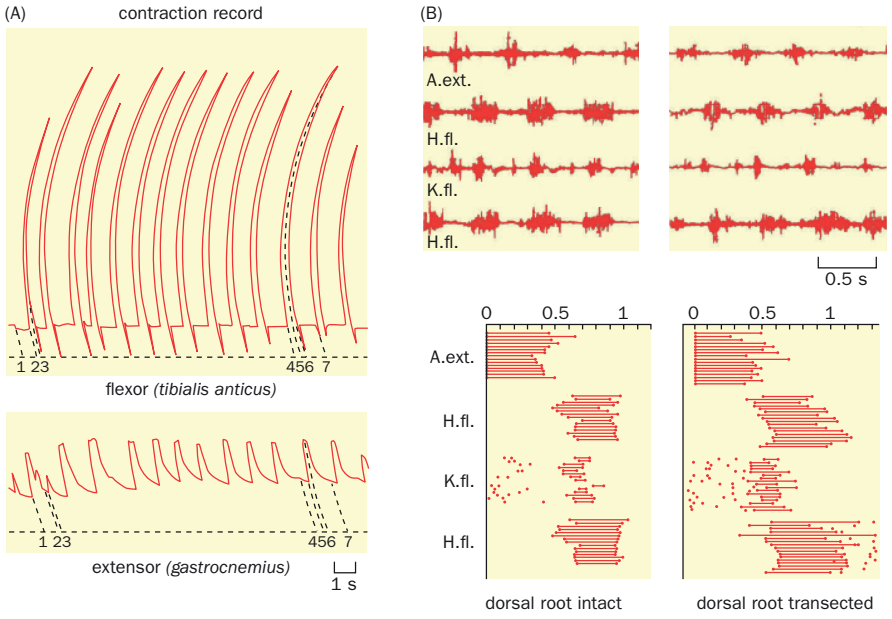

Figure 8-12 Rhythmic and coordinated muscle contraction in the absence of sensory feedback. (A) Contractions of a flexor muscle and an extensor muscle induced by spinal cord transection were recorded. Dorsal roots had been transected before the experiment to remove sensory feedback. The numbers and dashed lines below are used to synchronize the two records so the contraction of the two muscles can be compared in the same time frame. Within each cycle, the flexor contracted before the extensor, followed by a period when neither muscle contracted. Thus, rhythmic activation of these muscles persisted in the absence of sensory feedback. **(B)** A mesencephalic cat, in which the brainstem/spinal cord and the cerebral cortex/thalamus had been surgically disconnected, was induced to walk on a treadmill by brainstem stimulation (see Figure 8-17). Action potentials in four muscles of the same hind limb during the step cycle were recorded by electromyogram (EMG). The four muscles showed similar activity patterns when sensory feedback was intact (left) or removed by dorsal root transection (right), as seen in the EMG record (top) and in their timing of activation during the step cycles (bottom; 15 EMG recordings per muscle were compiled, with step cycle as the *x* axis unit). The four muscles, from top to bottom, are an ankle extensor, a hip flexor, a knee flexor, and a second hip flexor. (A, adapted from Graham Brown T [1911] *Proc R Soc London [B]* 84: 308–319. B, from Grillner S & Zangger P [1975] *Brain Res* 88:367–371. With permission from Elsevier Inc.)

stem; in this case, the spinal lesion initiated the rhythmic activity.) Contrary to prediction (2), however, this experiment revealed that rhythmic contractions persist in the absence of sensory feedback.

Further support for the idea that an autonomous spinal cord mechanism could produce rhythmic output came when technical advances in 1960–1970 made it possible to measure rhythmic contraction of many muscles during locomotion. For example, in a widely used experimental preparation, an incision is made at the level of the midbrain (mesencephalon; Figure 1-8) of a cat such that the cerebral cortex/thalamus and the brainstem/spinal cord are disconnected. Although the resulting "mesencephalic cat" can no longer voluntarily control its movement, it can still walk on a treadmill after brainstem stimulation. The contractions of many muscles during walking can be recorded simultaneously by their action potential patterns in electromyograms. The coordinated contractions of different leg muscles during stepping were found to be similar before and after dorsal root transection, as measured by the timing and duration of contraction for each muscle during the stepping cycle (Figure 8-12B).

Studies of rhythmic movements in invertebrate systems likewise found that rhythmicity originates from specific segments or ganglia in the central nervous system (see Section 8.5 below). Collectively, these experiments led to the concept of the **central pattern generator** (**CPG**), a central nervous system circuit capable of producing rhythmic output for coordinated contraction of different muscles without sensory feedback. The existence of CPGs does not mean that sensory feedback is unimportant. On the contrary, sensory feedback modulates and can override the CPG rhythm. For example, in the mesencephalic cat, sensory feedback produced by increasing the speed of the treadmill can modulate the speed of the stepping cycle and even trigger a transition of the motor patterns from walking to trotting or galloping. Nevertheless, experiments such as those described in Figure 8-12 indicate that rhythmic output can originate from neural circuits in the spinal cord upon initiation.

The concept of CPGs has extended beyond control of locomotion; CPGs have been proposed to control breathing (see Box 8-1), swallowing, and many other rhythmic movements. Indeed, the phenomenon of neural network oscillation goes beyond motor control. For example, different frequencies of rhythmic activity observed in the thalamus, cerebral cortex, and hippocampus have been proposed to play important roles in perception and cognition. How do neural circuits produce rhythmic output?

8.5 Intrinsic properties of neurons and their connection patterns produce rhythmic output in a model central pattern generator

Our best mechanistic understanding of rhythmic output production by CPGs has come from studies of invertebrate model circuits. These circuits usually consist of a small number of individually identifiable neurons that are large in size and easily accessible for intracellular recordings (Section 14.1). For example, the **stomatogastric ganglion** (**STG**) of crustaceans (lobster and crab) produces a pyloric rhythm to control the cyclic movement of a portion of the stomach. The pyloric rhythm can be seen in the triphasic firing patterns of four types of neurons—one interneuron (AB) and three types of motor neurons (PD, LP, and PY)—through simultaneous intracellular recordings (**Figure 8-13**A). Each neuron cycles between a hyperpolarized state and a depolarized state with bursts of action potentials. Importantly, the pattern seen in an intact lobster or crab can be faithfully reproduced when the stomatogastric nervous system is studied *in vitro* in the complete absence of sensory feedback, indicating that the rhythmic firing pattern is intrinsic to the STG.

The connection patterns between these four types of neurons (Figure 8-13B) have been determined by simultaneous electrophysiological recording and by cell ablation experiments. At the core of the pyloric rhythm is the AB interneuron, which exhibited rhythmic firing even when it was isolated from the rest of the circuit (Figure 8-13C). Thus, AB is a **pacemaker cell** which produces rhythmic output even in the absence of input. This pacemaker property results from the AB neuron's **intrinsic properties**, which are determined by the composition, concentration, and biophysical properties of the ion channels it expresses. Based on studies of other STG neurons, the transition from the depolarized state to the hyperpolarized state in AB is presumed to result from inactivation of voltage-gated cation channels and delayed opening of K^+ channels, much like the voltage-gated Na^+ and K^+ channels that underlie action potential production (Section 2.10). The rebound from the hyperpolarized state to the depolarized state likely results from opening of hyperpolarization-activated cation channels such as HCN channels (Figure 2-35), which causes depolarization, leading to activation of voltage-gated cation channels.

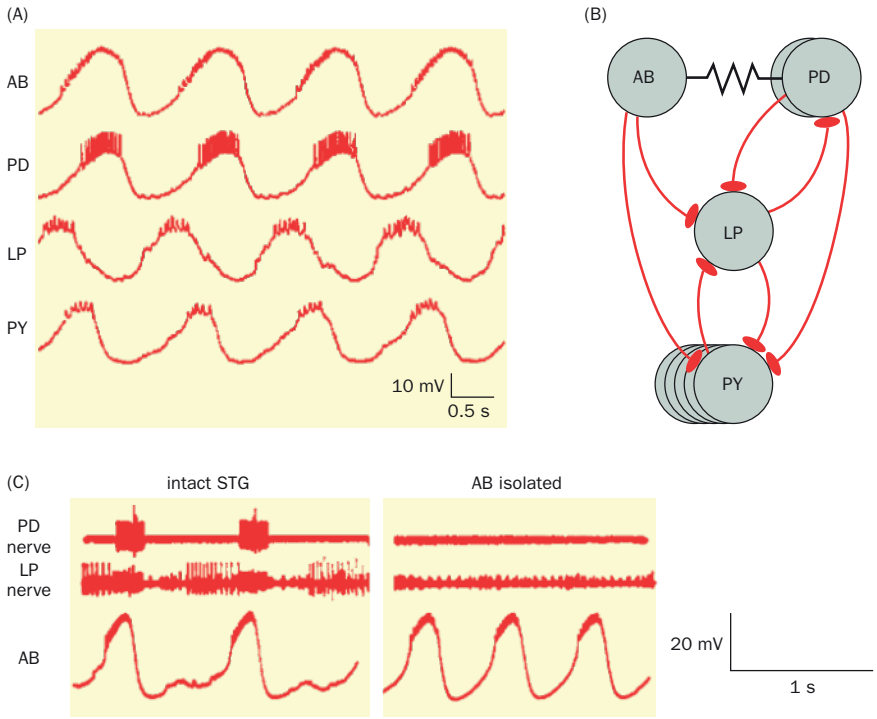

Figure 8-13 The pyloric circuit in the crustacean stomatogastric nervous system. (A) Simultaneous recordings of AB, PD, LP, and PY neurons in the stomatogastric ganglion (STG) show that each neuron cycles between depolarized and hyperpolarized states, with the AB/PD, LP, and PY neurons having offset activation phases. Action potentials (vertical spikes) are associated with the depolarized states. **(B)** The connection diagrams between 1 AB, 2 PD, 1 LP, and 5 PY neurons. AB and PD are electrically coupled through gap junctions (zigzag line). All chemical synapses are inhibitory. **(C)** In this experiment, the STG was first dissected out but remained connected with its central input nerve. The output spikes of PD and LP neurons were measured by extracellular recordings of their motor nerves, while the AB neuron was recorded by intracellular recording. All exhibited rhythmic output patterns (left). The conduction of the input nerve was then blocked, and the PD and LP neurons were ablated, as seen by the lack of spike output. The AB neuron continued to oscillate (albeit faster) in the absence of all functional connections (right). (A & B, adapted from Marder E & Bucher D [2007] *Ann Rev Physiol* 69:291–316. With permission from Annual Reviews. C, adapted from Miller JP & Selverston A [1982] *J Neurophysiol* 48:1378–1391.)

As diagrammed in Figure 8-13B, AB is electrically coupled to PD motor neurons through gap junctions; this causes PDs to fire in sync with AB. AB and PDs also form inhibitory chemical synapses onto LP and PYs, thereby inhibiting their firing. LP and PYs mutually inhibit each other; LP also inhibits PDs. Thus, when AB and PDs are in their depolarized state, their firing inhibits LP and PYs, forcing them to fire out of sync with AB/PDs. When AB/PDs stop firing, LP rebounds from inhibition before PY (this is because LP receives less inhibition from PDs and expresses fewer K^+ channels and more HCN channels than does PYs); at this point, LP inhibits firing of PDs and PYs. When the PYs eventually rebound from inhibition, they inhibit firing of LP, thereby disinhibiting PDs and facilitating the beginning of the next cycle. This chain of mutual inhibition among the three types of motor neurons produces the triphasic rhythm used to control coordinated contraction of the stomach muscles innervated by PD, LP, and PY neurons. In summary, the rhythmic firing of STG neurons is determined by the intrinsic properties of the constituent neurons as well as their connection patterns and strengths.

The simplicity of the crustacean STG system has enabled researchers to generate quantitative models based on the intrinsic properties of individual neurons and the connection strengths of the gap junction and inhibitory synapses. Such models have been used to simulate rhythmic output that matches experimental data. In one such study, the pyloric rhythm was simplified by lumping AB and PD together such that there are three neuronal types in the model: AB/PD, LP, and PY. From 20 million combinations of ion channel compositions (which determine membrane conductance) and connection strengths (which determine synaptic conductance) between the three types of neurons, nearly half a million distinct "solutions" that closely resembled the pyloric rhythm observed in animals were found. Two such solutions produced nearly identical triphasic rhythms (**Figure 8-14**, top), using notably different combinations of membrane and synaptic conductances (Figure 8-14, bottom). For example, the Na^+ conductance in the PY neuron is low in the case on the left and high in the case on the right, while the KCa conductance (reflecting the properties of Ca^{2+}-activated K^+ channels; Box 2-4) in the LP neuron is high on the left and low on the right. Variable parameters have

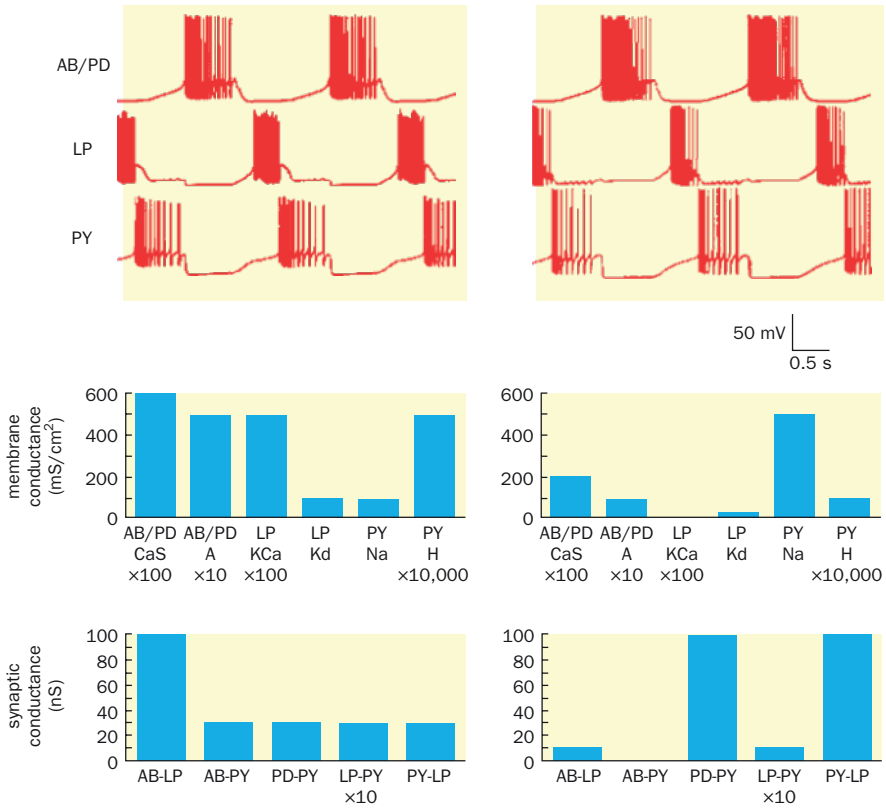

Figure 8-14 Similar network activity can be produced by distinct combinations of circuit parameters. Membrane potential traces from two model pyloric networks closely resemble each other (top), despite being produced by very different combinations of ion channels and synaptic strengths (bottom). Only a small subset of ion channel properties (represented as membrane conductance) and synaptic connection parameters (represented as synaptic conductance) are listed here. CaS, a voltage-gated slow and transient Ca^{2+} current; A, a voltage-gated transient K^+ current; KCa, a Ca^{2+}-dependent K^+ current; Kd, a delayed rectifier K^+ current; Na, a voltage-gated Na^+ current; H, a hyperpolarization-activated inward current. See Box 2-4 for more detail about the ion channels that produce some of these currents. (Adapted from Prinz AA, Bucher D, & Marder E [2004] *Nat Neurosci* 7: 1345–1352. With permission from Springer Nature.)

indeed been observed experimentally in natural populations of animals. Thus, distinct combinations of intrinsic neuronal properties and connection strengths can generate similar network properties, reflecting the flexibility and robustness of the network producing the pyloric rhythm. This finding suggests that the activity patterns of neurons and the network are *degenerate*, in that they can be achieved in multiple ways.

The crustacean STG system is also regulated by multiple neuromodulators, which act by changing membrane and synaptic conductances in specific neurons that express their receptors (Section 3.11; neuromodulation will be further discussed in Box 9-1). As many solutions produce similar rhythmic output patterns, each neuromodulator can in principle regulate a distinct set of ion channels or synaptic transmission components in different cells to help produce the same rhythmic output pattern.

8.6 The spinal cord uses multiple central pattern generators to control locomotion

The mechanisms by which CPGs in the vertebrate spinal cord control locomotion are more complex and less well understood than those of the crustacean STG. Nevertheless, insights obtained from less complex invertebrate circuits can be applied to test specific hypotheses. As discussed earlier, an elementary operation in motor coordination is the alternate contraction of the extensor and flexor controlling the same joint (Figure 8-8). In one model allowing this, the extensor and flexor motor neurons are each activated through mutually inhibitory premotor circuits (**Figure 8-15**A). At a higher level, different extensor–flexor pairs that control different joints of the same limb might be coordinated by analogous interactions among excitatory and inhibitory neurons to bring about coordinated movement of a limb; these constitute a CPG network for an individual limb. At an even higher level, CPG networks in the four limbs might be further coordinated to control different kinds of locomotion. For instance, during walking of most mammals, left and right limbs are out of sync, as are forelimbs and hind limbs on the same side. This may involve mutual inhibition of CPGs controlling these different limbs. Such models propose that mutual inhibition of left and right CPGs switches to mutual excitation during hopping or galloping so that left and right limbs are in sync (Figure 8-15B; Figure 8-11).

Physiological recording and perturbation experiments in preparations such as the mesencephalic cat have provided support for this conceptual framework of CPG organization. However, a deeper understanding of locomotion control requires identification of the constituent neurons and elucidation of the connection patterns of the CPG network, as has been achieved with the crustacean STG circuit. Since these CPG elements are composed of many individual neurons of multiple cell types, the methods that allowed researchers to crack the simpler STG circuit—such as simultaneous recording of multiple neurons and systematic ablation of identified neurons—are inadequate. The circuit functions performed by a single neuron in the STG are likely carried out by a specific type of neuronal populations in the vertebrate spinal cord. One promising approach is to use findings from gene expression and developmental studies (Figure 7-10) to gain genetic access to individual spinal neuron types. Genetic access could then allow connec-

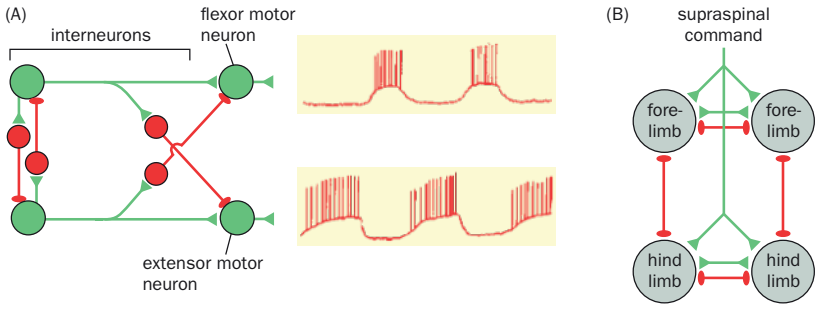

Figure 8-15 Conceptual framework for mammalian central pattern generators that control locomotion. (A) In this model (left), flexor and extensor motor pools (represented by single motor neurons) are excited by corresponding excitatory premotor neurons (green). These excitatory premotor neurons inhibit each other and their antagonistic motor neurons through inhibitory interneurons (red), thus creating alternating patterns of excitation (right). **(B)** At a higher level, CPG networks for different limbs are proposed to be connected via inhibitory (red) and excitatory (green) interactions. The excitatory and inhibitory interactions between limbs may be switched on or off, depending on modes of locomotion. All CPG networks also receive descending excitatory input from the brainstem and motor cortex. While serving as good working hypotheses, these models are hypothetical, as specific constituent neuronal elements have not yet been identified. (A, adapted from Pearson K [1976] *Sci Am* 235[6]:72–86. With permission from Springer Nature. B, adapted from Grillner S [2006] *Neuron* 52:751–766. With permission from Elsevier Inc.)

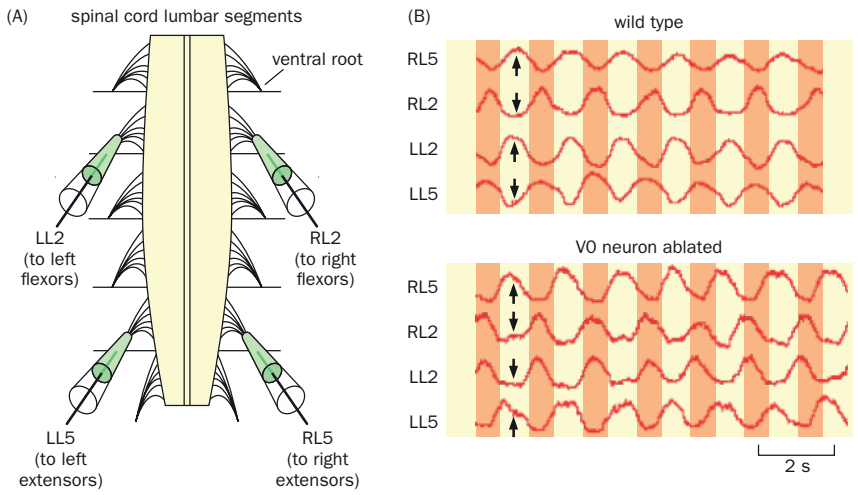

Figure 8-16 Ablation of V0 spinal cord interneurons disrupts left–right alternation. (A) Schematic of experimental setup. Simultaneous recordings of four ventral roots, which connect to extensors and flexors of hind limb muscles, as indicated, were performed in an *in vitro* explant. The locomotor-like pattern in this preparation was triggered by application of NMDA and serotonin, mimicking brainstem activation (Figure 8-17). **(B)** Top, in wild-type mice, the activities of left and right ventral roots of lumbar segment 2 (LL2 and RL2) alternated with each other, as did the activities of LL5 and RL5; these alternating activities account for the alternating movement of the left and right limbs during walking. Bottom, when V0 neurons were ablated, the activities of LL2 and RL2 synchronized, as did those of LL5 and RL5; this produced a hopping movement. Note that the activities of LL2 and LL5, and those of RL2 and RL5, also alternated because their flexor–extensor relationships remained unchanged when V0 was ablated. Dark and light alternating stripes represent the alternating phases of the locomotor cycles. (Adapted from Talpalar AE, Bouvier J, Borgius L, et al. [2013] *Nature* 500:85–88. With permission from Springer Nature.)

tivity tracing and activity manipulation of entire populations of specific neuronal cell types using modern neural circuit analysis tools (see Chapter 14).

We use one specific example to illustrate this approach. As discussed in Section 7.4, the transcription factor Dbx1 is expressed in developing spinal cord progenitors that eventually become V0 interneurons. Transgenic mice were produced in which Dbx1-expressing cells conditionally express diphtheria toxin A following Cre-induced recombination. These mice were crossed to a second transgenic mouse line in which Cre recombinase is expressed in the spinal cord, including Dbx1-expressing progenitors. The resulting double transgenic mice, in which spinal cord V0 neurons were specifically ablated by diphtheria toxin A expression, exhibited a striking phenotype: wild-type mice alternate their left and right limbs during walking, whereas transgenic mice synchronized their limbs such that they hopped rather than walked at all speeds tested (**Movie 8-4**). Recording the hind limb flexor and extensor activities in an *in vitro* spinal cord explant preparation indicated that the left–right alternating firing pattern was switched to a synchronous firing pattern (**Figure 8-16**). Thus, V0 interneurons play an essential role in alternating the activities of left and right limbs during normal walking. The flexor–extensor cycles within each limb remained intact despite the disruption of left–right alternation in the absence of V0 interneurons, suggesting that they are regulated independently.

V0 interneurons comprise both excitatory and inhibitory subpopulations. Interestingly, ablating inhibitory and excitatory V0 interneurons preferentially affected left–right alternation at low and high locomotion speeds, respectively. These observations suggest that different subpopulations are recruited to the same regulatory network for different locomotion speeds; in other words, the composition of CPGs regulating the same motor pattern is dynamic. Similar observations have been made in studies of zebrafish swimming on different molecularly identified neuronal subsets: as swimming speed increases, new interneuron populations become active, while those active during low speeds become inactive.

Recent studies have suggested that ventral spinal interneurons are highly heterogeneous, having diverse developmental origins, positions along the anterior–posterior axis, and gene expression patterns. For instance, spinal cord neurons derived from the V1 progenitor alone (Figure 7-10) may contain dozens of distinct subtypes. Functional interrogation of specific spinal interneuron subtypes, like that of the V0 interneuron discussed here, should provide new insight into how spinal cord circuits control movement.

8.7 The brainstem contains specific motor command nuclei

Although isolated spinal cord preparations can generate rhythmic output for locomotion, as discussed in Section 8.4, the initiation of rhythmic output requires excitatory stimuli, such as application of glutamate. Where does endogenous

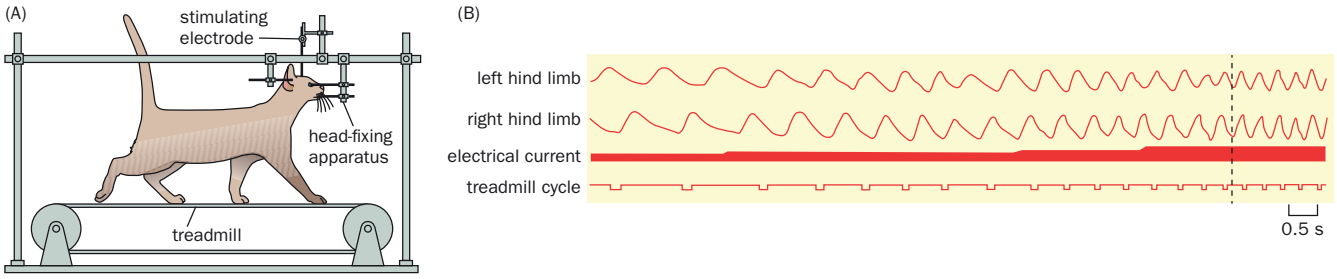

Figure 8-17 Electrical stimulation in the mesencephalic locomotor region (MLR) of the brainstem initiates stepping. (A) Experimental setup. An incision is made in the midbrain such that the cerebral cortex/thalamus is disconnected from the brainstem/spinal cord. The resulting mesencephalic cat cannot voluntarily control its locomotion. When placed on a treadmill with speed driven by the step cycle of the cat, electrical stimulation is applied to specific parts of the brain to initiate locomotion, which can be measured by limb movement and treadmill speed. **(B)** Electrically stimulating the MLR initiated movement, as seen in the cycles of the hind limbs. Furthermore, increasing the electrical stimulation current (thick trace below the hind limb cycles) sped up the step cycle, as seen in the increasing frequencies of the step cycles and treadmill cycle (bottom). Note that toward the end (after the vertical dashed line), trotting became galloping, with both hind limbs moving in sync. (Adapted from Shik ML, Severin FV, & Orlovski GN [1966] *Biophysics* 11:756–765. With permission from Springer Science & Business Media.)

excitation come from? Electrical stimulation of an area called the **mesencephalic locomotor region** (**MLR**) in the brainstem was found to initiate locomotion in mesencephalic cats. Indeed, increasing the intensity of MLR stimulation could speed up the walking and trigger transitions to trotting or galloping (**Figure 8-17**). Thus, the MLR appears to be a brainstem center that controls locomotion. MLR stimulation activates other brainstem neurons, which in turn send descending axons through the reticulospinal tract to innervate spinal interneurons and motor neurons.

Classic electrical stimulation, lesion, and anatomical tracing studies are limited by a lack of cellular resolution, as they are not restricted to specific cell types. As in the case of spinal cord CPG research, recent advances in neural circuit dissection have begun to change this picture. After locating the MLR in the midbrain of a head-fixed mouse, where electrical stimulation could facilitate locomotion, researchers resorted to optogenetic activation of neurons in that region with specific transmitter types by expressing channelrhodopsin (ChR2) only in cholinergic, GABAergic, or glutamatergic neurons. They found that photoactivating glutamatergic neurons (but not the other classes) could initiate or speed up locomotion (**Figure 8-18**A). Conversely, optogenetic inhibition of MLR gluta-

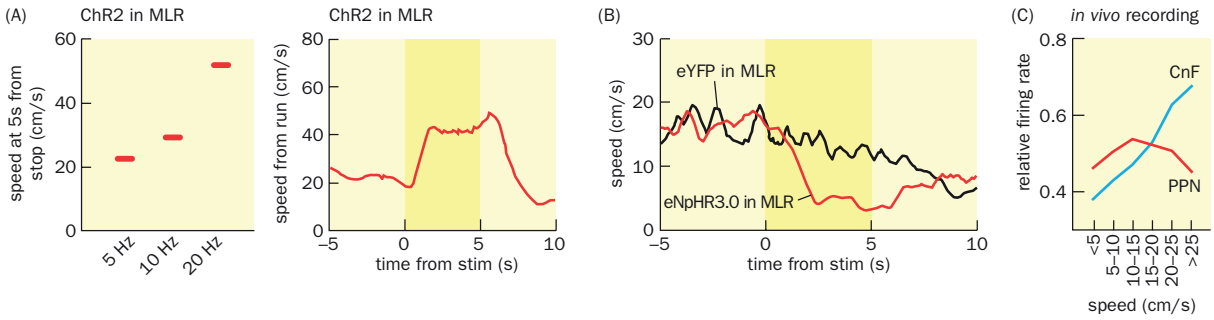

Figure 8-18 Dissecting the mouse mesencephalic locomotor region. (A) Left, optogenetic stimulation of channelrhodopsin- (ChR2-) expressing glutamatergic neurons in the MLR initiates locomotion from rest, the speed of which positively correlates with stimulation frequency. Right, optogenetic activation of these neurons also increases the speed of moving mice. **(B)** Optogenetic stimulation of halorhodopsin- (eNpHR3.0-) expressing MLR glutamatergic neurons, which silences their activity (Section 14.25), reduces the speed of locomotion. As a control, optogenetic stimulation of eYFP-expressing MLR glutamatergic neurons has no effect. **(C)** *In vivo* extracellular recordings of glutamatergic neurons (identified using a phototagging strategy; see Section 14.20 for details). Glutamatergic neurons in the cuneiform nucleus (CnF) have higher firing rates (relative to baseline) than those in the pedunculopontine nucleus (PPN) during high-speed locomotion, and the converse is true during low-speed locomotion. (A & B, from Roseberry TK, Lee AM, Laline AL, et al. [2016] *Cell* 164:526–537. With permission from Elsevier Inc. C, from Caggiano V, Leiras R, Goñi-Erro H, et al. [2018] *Nature* 553:455–460. With permission from Springer Nature. See also Josset N, Roussel M, Lemieux M, et al. [2018] *Curr Biol* 28:884–901; Capelli P, Pivetta C, Esposito MS, et al. [2017] *Nature* 551:373–377.)

matergic neurons slowed locomotion (Figure 8-18B). Further dissection of specific subregions within the MLR identified glutamatergic neurons from a dorsal cuneiform nucleus (CnF) as a major driver of high-speed locomotion, whereas glutamatergic neurons from a ventral pedunculopontine nucleus (PPN) appeared to drive slow gaits. *In vivo* extracellular recordings revealed that CnF and PPN glutamatergic neurons are preferentially active during locomotion at high and low speeds, respectively (Figure 8-18C). Taken together, these experiments suggest that glutamatergic neurons in the MLR (particularly the CnF) promote locomotion. Further experiments identified glutamatergic neurons in the lateral paragigantocellular nucleus, a small nucleus in the caudal brainstem, as an intermediate between the MLR and spinal cord that controls high-speed locomotion.

In addition to controlling locomotion, the brainstem also contains myriad neuronal groups that control many other bodily movements. For example, recent studies using modern circuit analysis tools have identified glutamatergic neurons in a brainstem nucleus called MdV (standing for medullary reticular formation, ventral part) that preferentially provide direct input to motor neurons controlling forelimb but not hind limb muscles, and thereby regulate skilled forelimb-based motor tasks. Additional brainstem nuclei regulate eye movement, licking, chewing, swallowing, whisking (a prominent behavior for rodents), and breathing. We discuss breathing in **Box 8-1** as another example of a brainstem motor control circuit.

Box 8-1: How is breathing controlled?

From birth to death, animals must breathe continually, inhaling oxygen and exhaling carbon dioxide in order to maintain metabolic activity. While we do it without thinking much of the time, breathing can be under voluntary control (think of divers and opera singers). In mammals, a typical breath at rest consists of an inspiratory phase involving active contraction of muscles that control the diaphragm, followed by an expiratory phase. As metabolism increases (as when exercising), expiration muscles are recruited to produce active expiration to empty the lung so that the next inspiration can take in more air more quickly. Furthermore, there can be a third phase termed *post-inspiration*, an expiratory phase that slows the release of air through the active contraction of upper airway muscles (useful for singing long syllables, for example). The three phases are controlled by three interacting oscillator circuits located in nearby regions of the medulla (**Figure 8-19**A, B). We focus our discussion here on the region that controls the inspiratory phase, the **pre-Bötzinger complex** (**preBötC**), which is the best studied of the three.

The preBötC was discovered as a center that generates breathing rhythms in the early 1990s by systematic anatomical mapping. In a reduced neonatal rat preparation that includes brainstem and spinal cord, rhythmic output reflecting breathing cycles can be recorded from several nerves, including the hypoglossal nerve (cranial nerve XII, which innervates tongue muscles) and phrenic nerve (a cervical nerve that innervates the diaphragm). Researchers then sectioned away brain regions from the reduced preparation and found that removing sections rostral or dorsal to preBötC did not affect rhythmic output, but if the region containing the preBötC was sectioned away, rhythmic output was abolished. Importantly, a ~500 μm coronal slice containing the preBötC was sufficient to produce rhythmic activity in the hypoglossal nerve, and whole-cell recordings confirmed that neurons within the preBötC produced rhythmic burst firing (Figure 8-19C). Further studies revealed that preBötC axons control inspiration by activating premotor neurons in the rostral ventral respiratory group (rVRG; Figure 8-19B), which activates inspiratory motor neurons that control diaphragm contraction.

The neural mechanisms underlying rhythm generation have not yet been resolved despite intense effort, in part due to the complexity and heterogeneity of preBötC neurons. Essential for rhythm generation are a few thousand excitatory neurons derived from progenitors that express the transcription factor Dbx1 (the same gene expressed by progenitors of V0 interneurons in the spinal cord; Figure 8-16; Figure 7-10). In *Dbx1* mutant mice, these preBötC neurons fail to develop, and mice die at birth because they cannot breathe. Indeed, rhythmic activation of preBötC neurons could be detected several days before pups were born in control but not *Dbx1* mutant slices using electrophysical recordings and Ca^{2+} imaging (**Figure 8-20**A). Furthermore, optogenetic activation of channelrhodopsin-expressing preBötC neurons derived from $Dbx1^{+}$ progenitors could shift the phase or increase the magnitude of inspiration, depending on the timing of photostimulation within the breathing cycle (Figure 8-20B). Together, these experiments reveal a central role played by $Dbx1^{+}$ progenitor–derived preBötC neurons in the generation of inspiration. *In vivo* single-unit recordings revealed further heterogeneity of these neurons, some of which fired just before inspiration, while others fired during or after inspiration. A current model posits that among $Dbx1^{+}$ progenitor–derived preBötC neurons, some are involved in rhythmogenesis, whereas others send output to premotor neurons to execute the breathing pattern.

(*Continued*)

Box 8-1: continued

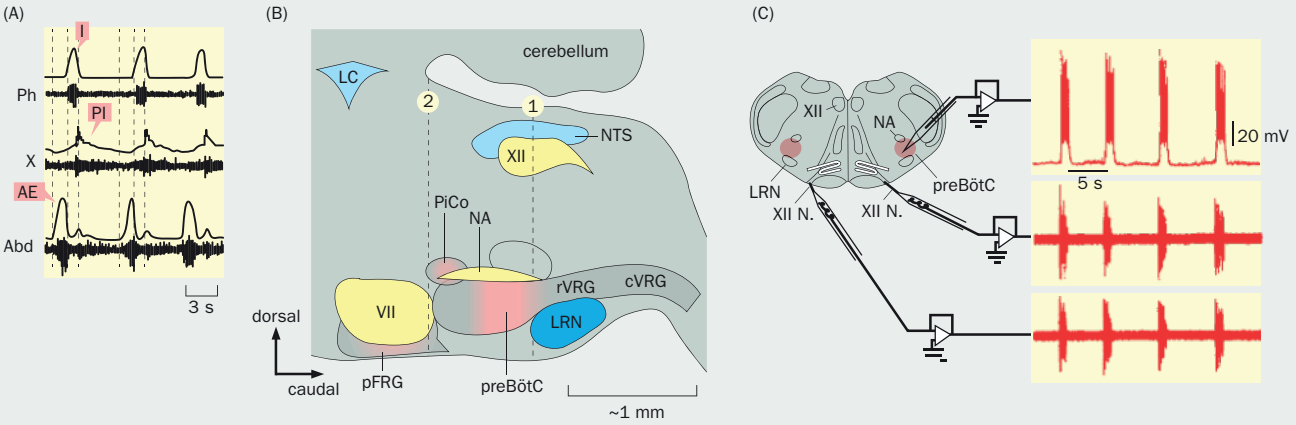

Figure 8-19 Brainstem nuclei that control breathing. (A) Breathing cycles consisted of three phases, inspiration (I), post-inspiration (PI), and active expiration (AE), shown here in a reduced rat preparation. The three phases were measured via electrical recordings from the phrenic (Ph) nerve, cranial nerve X, and lumbar abdominal (Abd) nerve, respectively; raw spike patterns (bottom) and spike rates (top) are shown. Vertical dashed lines separate the three phases for two cycles. Breathing cycles can also consist of the following combinations of active phases: I, I + PI, or I + AE. **(B)** A sagittal schematic of the rat brainstem. Nuclei that control breathing phases are highlighted in red: the pre-Bötzinger (preBötC) for inspiration, post-inspiratory complex (PiCo) for post-inspiration, and parafacial respiratory group (pFRG) for active expiration. The rostral ventral respiratory group (rVRG) contains inspiratory premotor neurons that receive input from the preBötC. The caudal ventral respiratory group (cVRG) contains expiratory premotor neurons that receive input from the pFRG. Other labeled anatomical landmarks are the locus coeruleus (LC), which contains norepinephrine modulatory neurons; cranial nuclei VII and XII, which contain motor neurons innervating the face and tongue, respectively; nucleus of solitary tract (NTS), which relays taste and interoceptive (for example, lung mechanosensory) information to higher brain centers; nucleus ambiguous (NA), which contains motor neurons that control the larynx, pharynx, and soft palate for swallowing and speech; and lateral reticular nucleus (LRN), which relays input to the cerebellum. **(C)** Schematic (left) and recordings (right) from a coronal slice containing the preBötC. Rhythmic burst firing of cranial nerve XII (XII N.; bottom two traces) and of a neuron within the preBötC are detected via extracellular recording and whole-cell recording, respectively. IO, inferior olive, which sends climbing fiber projections to the cerebellum (Section 8.10). (A & B, from Del Negro CA, Funk GD, & Feldman JL [2018] *Nat Rev Neurosci* 19:351–367. With permission from Springer Nature. C, from Smith JC, Ellenberger HH, Ballanyi K, et al. [1991] *Science* 254:726–729. With permission from AAAS.)

Recent genetic dissection of preBötC neurons has also revealed subsets that serve specialized functions. For example, a subset of Dbx1^{+} progenitor–derived preBötC neurons sends ascending axons to the locus coeruleus (Figure 8-19B), where they synapse onto norepinephrine neurons to regulate brain states such as arousal and placidity (see Box 9-1 for more details on norepinephrine neurons). Another group of preBötC neurons receives neuropeptide input and con-

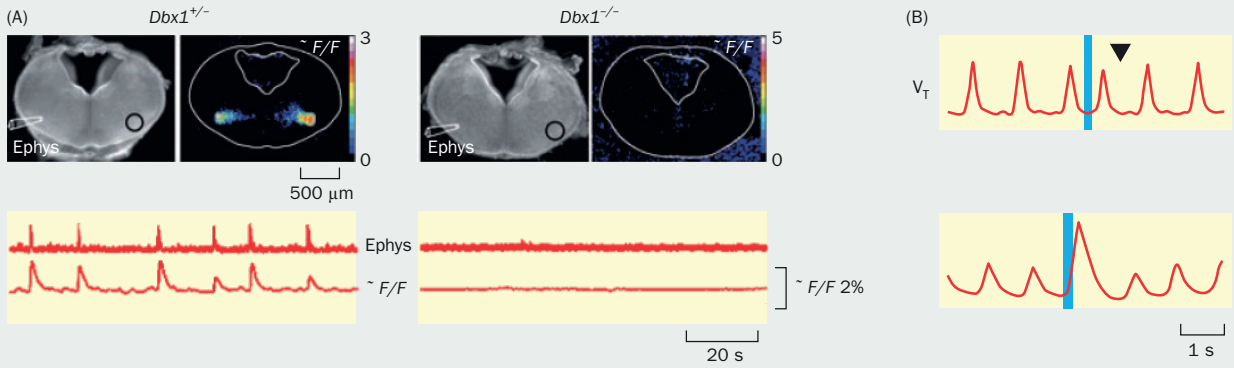

Figure 8-20 Dbx1^{+} progenitor–derived preBötC neurons control inspiration. (A) Top, micrographs of coronal slices from heterozygous control (left) and homozygous *Dbx1* mutant (right) embryonic day 15.5 pups. Within each pair, the bright-field images (left) show the extracellular electrophysiological recording site (Ephys) within the preBötC (circles on the right hemispheres). The fluorescence images (right) show elevated bulk Ca^{2+} signal, indicating active preBötC neurons. Bottom, traces of simultaneous electrophysiological recording and Ca^{2+} imaging show rhythmic activity of the preBötC. $\Delta F/F$, change in fluorescence signal divided by baseline fluorescence. **(B)** Tidal volume (V_T) of airflow measured in a transgenic mouse expressing channelrhodopsin in neurons derived from Dbx1^{+} progenitors. Top, when photostimulation was applied in the middle of the expiration phase, the next breathing cycle was shifted forward (downward arrowhead indicates where the next cycle would have been without the photostimulus). Bottom, when photostimulation was applied at the beginning of an inspiration, the magnitude of the inspiration increased. (A, from Bouvier J, Thoby-Brisson M, Renier N, et al. [2010] *Nat Neurosci* 13:1066–1074. With permission from Springer Nature. B, from Cui Y, Kam K, Sherman D, et al. [2016] *Neuron* 91:602–624. With permission from Elsevier.)

Box 8-1: continued

trols sigh, a double-sized breath induced by physiological needs, such as reinflating collapsed alveoli in the lung, or by emotions, such as sadness or relief. Breathing rhythms also interact intimately with other orofacial activities, such as swallowing, licking, whisking (for rodents), and speech (for humans). Some rhythmic movements, such as whisking and licking, are coordinated with breathing, and it has been proposed that the preBötC-based inspiratory rhythm may function as a master clock to regulate other rhythmic orofacial movements in order to coordinate distinct motor outputs. For example, inspiration and swallowing do not occur simultaneously to ensure that food does not accidentally enter the airway. Thus, investigation into the neural mechanisms of breathing can help understand many aspects of motor control as well as their interactions with higher brain centers involved in arousal and emotional regulation.

8.8 The basal ganglia consist of two parallel pathways that are oppositely regulated by dopamine

So far, we have followed the motor system along a direction opposite to the information flow for motor execution: from muscles to motor neurons, premotor neurons in the spinal cord, and brainstem motor command centers. However, as seen from Figure 8-2, the motor system is far from a linear feedforward path from central to peripheral. There is sensory feedback at each stage. Moreover, within each stage there are local recurrent loops (e.g., Figure 8-15). In the next few sections, we will study higher motor control regions, including the basal ganglia, thalamus, cerebellum, and neocortex. Long-range recurrent loops between these regions are essential features for motor control (Figure 8-2). We discuss these regions one by one, but need to bear in mind their close interactions. Importantly, each of these regions employs generic circuit architecture for functions beyond motor control; nevertheless, our understanding of how basal ganglia and cerebellar circuits operate has come mostly from studies of motor control. We begin with the basal ganglia.

The **basal ganglia** are a collection of nuclei interior to the cerebral cortex (Figure 1-8). Two neurological disorders, Parkinson's disease and Huntington's disease, which primarily affect the basal ganglia, highlight the importance of these structures in motor control. Patients with Parkinson's disease have difficulty initiating movement, while patients with Huntington's disease cannot stop excessive movement. (We will discuss these diseases in more detail in Chapter 12.) The basal ganglia use a generic circuit design (**Figure 8-21**) for a wide range of functions that vary according to the specific sources of input and output. Before discussing its function in motor control, we first outline the basal ganglia circuit.

The input nucleus of the basal ganglia is the **striatum**, also called the caudate-putamen because in primates the striatum consists of two separable structures, the caudate and the putamen. The striatum receives convergent excitatory input from the neocortex and the thalamus. The dorsolateral striatum preferentially receives input from sensory and motor cortices and thus is most directly involved in motor control. The dorsomedial striatum preferentially receives input from association cortices and is involved in cognitive processes. The ventral striatum (also called the **nucleus accumbens**) preferentially receives input from the prefrontal cortex, hippocampus, and amygdala, and regulates motivated behavior.

The great majority of neurons in the striatum are two types of intermingled GABAergic **spiny projection neurons** (SPNs; also called medium spiny neurons) distinguished by their expression of different G-protein-coupled dopamine receptors. Those expressing the D_1 receptor constitute the **direct pathway**, which projects predominantly to the output nuclei of the basal ganglia—the **globus pallidus internal segment** (**GPi**) and the **substantia nigra pars reticulata** (**SNr**). Those expressing the D_2 receptor constitute the **indirect pathway**, which projects predominantly to the **globus pallidus external segment** (**GPe**), which in turn sends GABAergic input to the GPi either directly or through the **subthalamic nucleus** (**STN**) (Figure 8-21A). The two pathways can be visualized in transgenic mice expressing green fluorescence protein (GFP) under the control of regulatory elements from the D_1 or D_2 dopamine receptor genes (Figure 8-21B). GPi and SNr

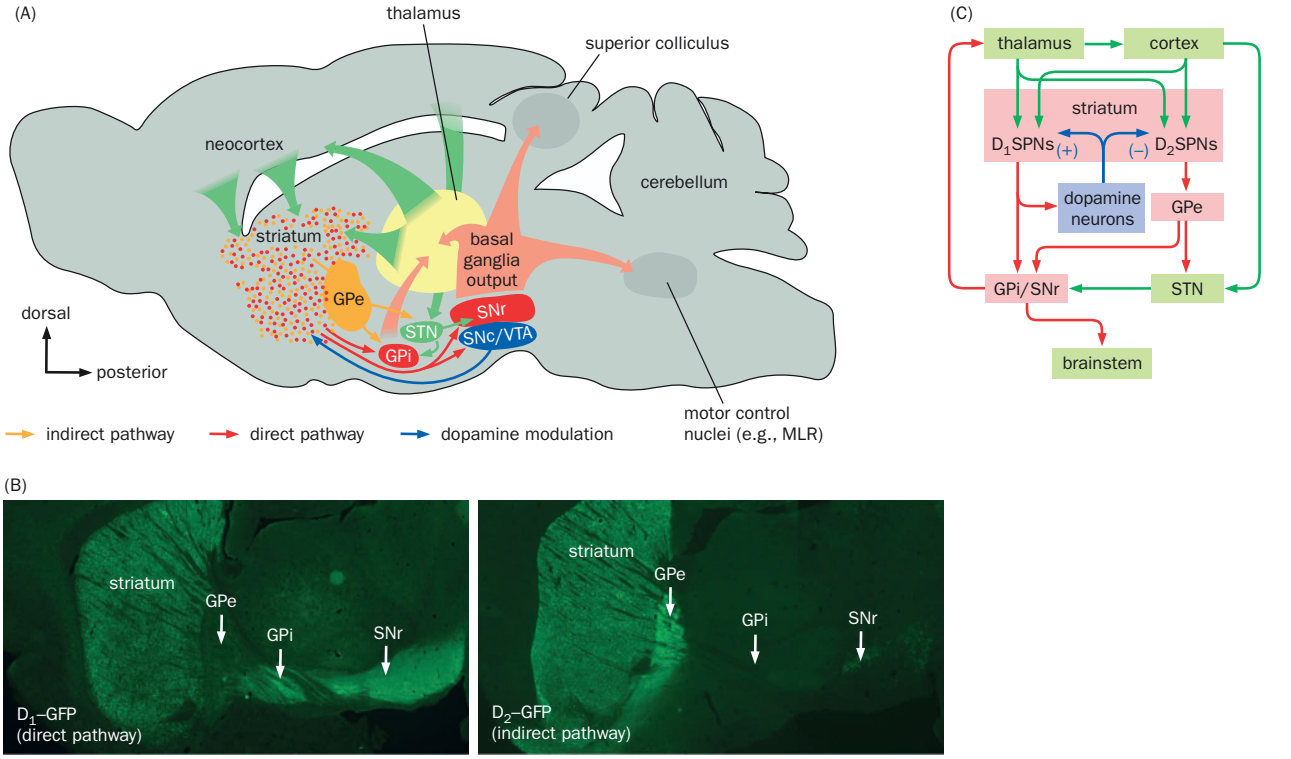

Figure 8-21 Organization of basal ganglia circuits. (A) A simplified model of basal ganglia circuits from a sagittal perspective of a mouse brain. The striatum receives excitatory inputs from the neocortex and thalamus and sends output via two types of GABAergic spiny projection neurons (SPNs). SPNs expressing the D_1 dopamine receptor (D_1SPN, red) constitute the direct pathway and project mainly to the globus pallidus internal segment (GPi) and substantia nigra pars reticulata (SNr). SPNs expressing the D_2 dopamine receptor (D_2SPN, orange) constitute mainly the indirect pathway and project to the globus pallidus external segment (GPe). The GPe sends GABAergic projections to the GPi and the subthalamic nucleus (STN, which also receives direct cortical input), which in turn projects to the GPi and SNr. The GPi and SNr send basal ganglia output to the thalamus, superior colliculus, and brainstem motor control nuclei, such as the mesencephalic locomotor region (MLR). Dopamine neurons in the substantia nigra pars compacta (SNc) and ventral tegmental area (VTA) also receive input from D_1SPNs and many other brain regions (not shown here) and send modulatory output back to the striatum. **(B)** The projection patterns of D_1SPNs (left) and D_2SPNs (right) are visualized in sagittal sections of transgenic mice in which green fluorescent protein (GFP) expression is driven by the regulatory elements of the D_1 and D_2 receptors, respectively. Cell bodies of both neuronal types are within the striatum; D_1SPNs project mainly to the GPi and SNr, whereas D_2SPNs project to the GPe, as seen by GFP fluorescence intensity. **(C)** A simplified basal ganglia circuit diagram. Green arrows represent excitatory projections. Red arrows represent inhibitory projections. Blue arrows represent dopaminergic projections, which promote D_1SPN (+) firing and inhibit D_2SPN (–) firing. (A & B, adapted from Gerfen CR & Surmeier DJ [2011] *Ann Rev Neurosci* 34:441–466. With permission from Annual Reviews.)

GABAergic projections target the thalamus, which itself projects to the neocortex and directly back to the striatum, forming two feedback loops (Figure 8-21A, C). The SNr also sends output to brainstem motor control nuclei and the superior colliculus. The actual connection patterns are more complex than the simplified model outlined here, but the model captures the major features of the basal ganglia circuit.

Dopamine modulates the excitatory synaptic connections through which the neocortex and thalamus provide input to striatal spiny projection neurons (see Box 9-1 for a general discussion of neuromodulatory systems). The dopamine neurons responsible for this modulation are located in the **substantia nigra pars compacta** (**SNc**) and the adjacent **ventral tegmental area** (**VTA**), which project preferentially to the dorsal and ventral striatum, respectively. Dopamine release has opposite effects on the direct and indirect pathways. Activation of the D_1 receptor, which is coupled to a stimulatory G protein, depolarizes D_1 receptor–expressing spiny projection neurons (D_1SPNs), activating the direct pathway. Activation of the D_2 receptor, which is coupled to an inhibitory G protein, hyperpolarizes D_2 receptor–expressing spiny projection neurons (D_2SPNs), inhibiting the indirect

pathway (Figure 8-21C). The activity of SNc/VTA dopamine neurons is in turn regulated by inputs from many brain regions, including direct input from D_1SPNs (Figure 8-21A, C).

8.9 The direct and indirect pathways act in concert to facilitate the selection and initiation of motor programs

Given the circuit properties discussed in Section 8.8, how do the basal ganglia regulate movement? *In vivo* recording studies indicate that striatal SPNs are mostly silent at rest. By contrast, output neurons in the GPi and SNr are active at rest, sending **tonic** inhibitory output to their targets. (Tonic refers to regularly timed and repetitive firing patterns; **phasic** refers to rapid and transient firing patterns.) Immediately before the onset of voluntary movement, cortical and thalamic excitatory input activates spiny projection neurons (e.g., **Figure 8-22**). This inhibits firing of GPi and SNr output neurons through the direct pathway, causing disinhibition of motor control centers in the superior colliculus and brainstem (Figure 8-21C), thus facilitating movement initiation. Likewise, tonic inhibitory output to the thalamus is also relieved, further promoting movement initiation. Early recording studies did not distinguish between D_1SPNs and D_2SPNs, and the interpretation of their findings is based on the projection patterns of D_1SPNs. Given their opposing roles in the circuit and regulation by dopamine, how do these two types of SPNs contribute to motor control?

Optogenetics (Section 14.25) has been used to test the causal relationship between movement and activation of the direct or indirect pathways. Channelrhodopsin was expressed in D_1SPNs or D_2SPNs in separate mice such that they could be activated by light. As predicted from the circuit model, activation of the direct and indirect pathways decreased or increased, respectively, the firing of SNr output neurons (**Figure 8-23**A). Behaviorally, direct pathway activation enhanced locomotion, whereas indirect pathway activation suppressed locomotion (Figure 8-23B). These experiments suggest that *global* activation of the basal ganglia direct or indirect pathway facilitates or inhibits movement, respectively.

Recent cell-type-specific *in vivo* recording revealed that both direct and indirect pathways are activated when animals initiate a specific motor behavior such as locomotion, suggesting a more nuanced picture than the simple idea that D_1SPNs promote movement while D_2SPNs inhibit movement. In one such experiment (**Figure 8-24**A), mice moved freely in an arena while Ca^{2+} imaging was performed on D_1SPNs or D_2SPNs via a head-mounted miniaturized microscope (see Section 14.22 for details). Body acceleration correlated positively with Ca^{2+} transients in both D_1 and D_2SPNs (Figure 8-24B). Furthermore, activity of individual D_1SPNs or D_2SPNs was selective for specific actions, such as acceleration, deceleration, and turning (Figure 8-24C). In a complementary experiment, bulk Ca^{2+} signals from D_1SPN or D_2SPN populations were recorded simultaneously using a technique called **fiber photometry** (Section 14.22) in freely moving mice; the behavior of mice was segmented into specific "syllables" based on their three-dimensional movements (Figure 8-24D). While both D_1 SPNs and D_2SPNs were generally activated by syllable onset, onset of certain syllables exhibited *temporal differences* between these two neuronal populations (Figure 8-24E).

Together, these experiments suggest that striatal SPNs in the direct and indirect pathways act in concert to regulate many aspects of motor behavior. That activity changes of SPNs correspond to onset of behavioral changes supports their function in the selection and initiation of specific motor programs. Antagonism between the direct and indirect pathways, as predicted by basal ganglia circuitry (Figure 8-21C), could manifest at different levels: global movement (for example, go versus no-go), selection of specific motor programs and simultaneous inhibition of other competing programs, and fine temporal regulation within a specific motor program. Future physiological recordings and temporally precise manipulations of direct and indirect pathway neurons specific for particular motor programs, in conjunction with precise behavioral monitoring, will shed more light on how the basal ganglia regulate movement.

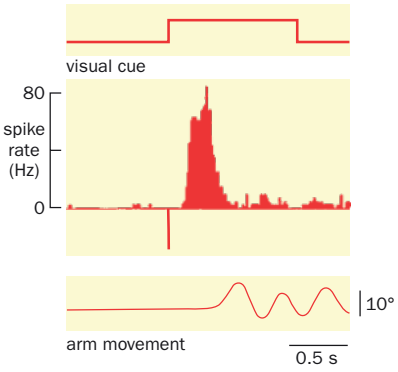

Figure 8-22 Firing of some striatal neurons anticipates movement onset. In this experiment, a monkey was trained to move its arm three times (bottom trace) in response to onset of a visual cue (top trace). The firing rate of a neuron in the arm control region of the striatum was recorded by an extracellular electrode. This striatal neuron did not track movement per se, but instead fired most vigorously *prior to* movement onset. Other striatal neurons in the same study did track movement (not shown). (Adapted from Kimura M [1990] *J Neurophysiol* 63:1277–1296.)

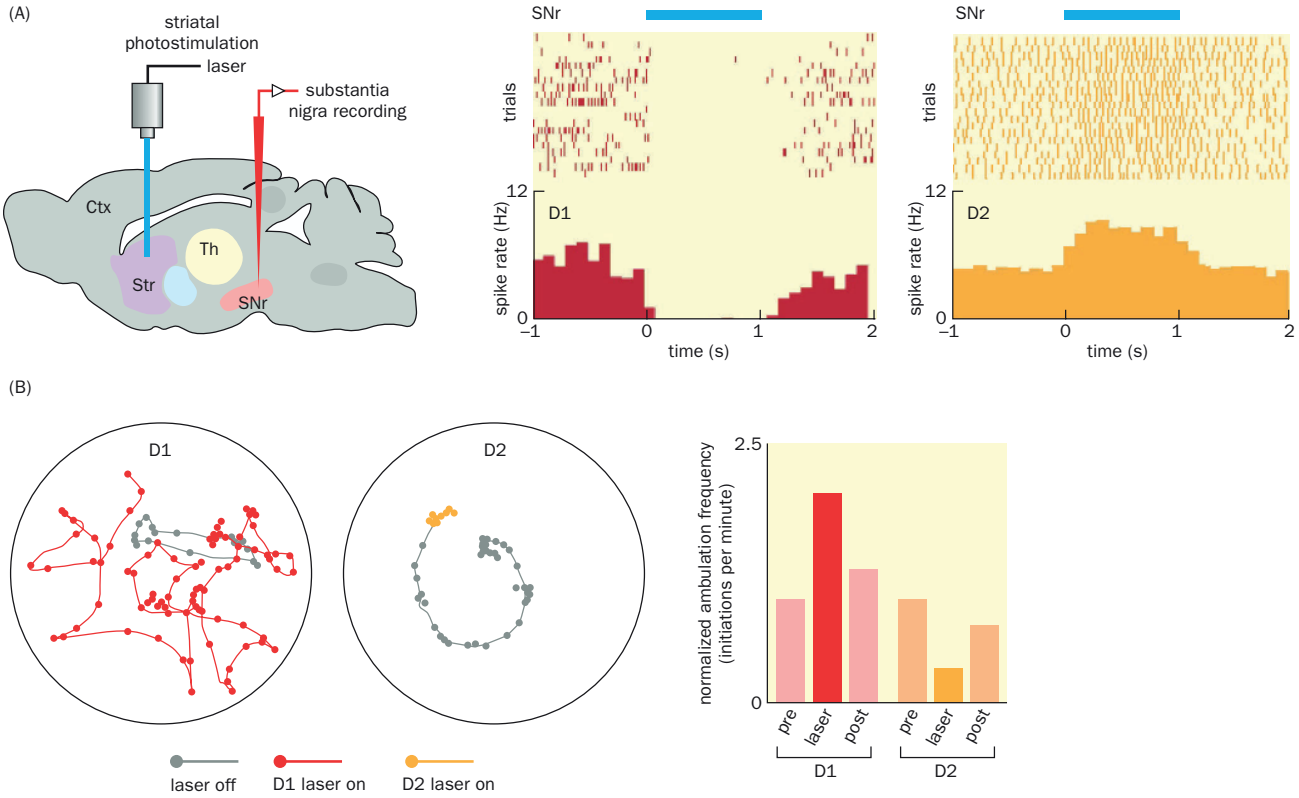

Figure 8-23 Function of the direct and indirect pathways investigated by optogenetic stimulation. (A) Left, schematic of the experiment depicted in a sagittal perspective of the mouse brain. Channelrhodopsin (ChR2) was specifically expressed in D_1SPNs or D_2SPNs in the striatum (Str). Middle and right, the top graphs are spike trains in which each row represents a trial; the bottom graphs illustrate the spike rate of the SNr neurons before, during, and after photostimulation. Photostimulation (blue bar) of D_1SPNs suppressed SNr neuron firing (middle panels), while stimulation of D_2SPNs increased SNr neuron firing (right panels). Ctx, cortex; Th, thalamus. **(B)** Photostimulation of D_1SPNs or D_2SPNs promotes or suppresses movement, respectively. The location of a mouse in a circular arena is measured at 300-ms intervals. The gray paths represent 20 s of activity before photostimulation; the colored paths (red or orange) represent 20 s of activity during photostimulation. When D_1SPNs were activated, the mouse moved more, as indicated by longer distances between the red dots. When D_2SPNs were activated, the mouse moved less, as indicated by the clustered orange dots. These effects are quantified in the right panel. (Adapted from Kravitz AV, Freeze BS, Parker PR, et al. [2010] *Nature* 466:622–626. With permission from Springer Nature.)

SNc dopamine neurons, which project to the dorsal striatum, have traditionally been thought to exhibit a tonic firing pattern for modulating striatal neuronal responses to excitatory input from cortex and thalamus. Recent *in vivo* recording and imaging experiments in behaving mice indicate that they too exhibit phasic firing preceding movement onset. Optogenetic manipulations suggest that SNc dopamine neurons promote initiation and vigor (for example, speed and amplitude) of subsequent movement. In addition to modulating movement, dopamine also regulates connection strengths of synapses between thalamic/cortical input and SPNs, which likely plays important roles in motor skill learning and habit formation. Dopaminergic projections from the VTA (which neighbors the SNc) to the ventral striatum are particularly important in carrying signals related to reward. We will return to the function of the basal ganglia when studying reward-based learning in Chapter 11 and movement disorders and addiction in Chapter 12.

8.10 The cerebellum contains more than half of all neurons in the brain and has a crystalline organization

The cerebellum (Latin for "little brain") is evolutionarily ancient in vertebrates and occupies a sizable chunk of the mammalian brain (Figure 1-8). Like the basal ganglia, the cerebellum has a generic circuit design that serves diverse functions. However, its best-characterized functions are fine control of movement and motor learning. Cerebellar defects in human patients and experimental animals cause

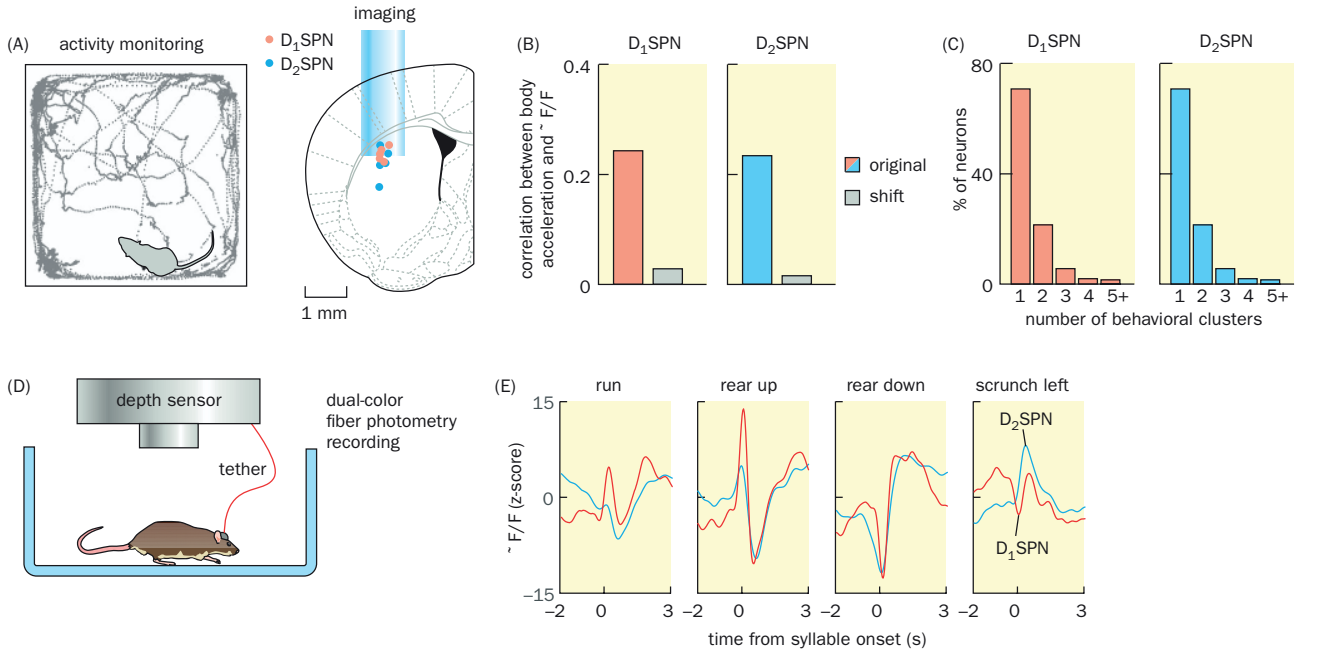

Figure 8-24 Measuring the activity of D_1SPNs or D_2SPNs during motor behavior. (A) Left, schematic of the experimental setup. Mice wearing a head-mounted microscope moved freely in an arena. Activity of D_1SPNs or D_2SPNs in dorsolateral striatum was imaged through a graded index (GRIN) lens via transgenic expression of the genetically encoded Ca^{2+} indicator GCaMP6 (Figure 14.41). **(B)** Analysis of time-dependent traces of body movement and Ca^{2+} signals in individual cells (as fluorescence change over baseline fluorescence, or $\Delta F/F$) indicated that the activity of both D_1SPNs and D_2SPNs are positively correlated with body acceleration (red and blue bars). As a negative control, when the two traces were temporally shifted, the correlations disappear (gray bars). **(C)** Activity of most individual D_1SPNs and D_2SPNs was selective for one or two specific actions, represented by "behavioral clusters" generated by quantitative analysis of behavior from continuous videos. **(D)** Schematic of dual-color fiber photometry recording of bulk Ca^{2+} activity in dorsolateral striatum of freely moving mice monitored by a sensor that records mouse three-dimensional movement. GCaMP6 and RCaMP1 (Ca^{2+} indicators with green and red fluorescence, respectively) were expressed in D_1SPNs and D_2SPNs, respectively. **(E)** Mouse behavior was segmented into syllables using an unsupervised machine-learning procedure (see Figure 14-52 for more detail; the descriptors on top reflect human observers' attempts to describe these syllables). D_1SPNs and D_2SPNs are generally activated at the onset of specific syllables. However, temporal differences between the activity of D_1SPNs and D_2SPNs were observed. For instance, the onset of "run" coincides with an increase in D_1SPN activity but a decrease in D_2SPN activity followed by an increase. Z-score is the difference from the mean divided by the standard deviation. (A–C, from Klaus A, Martins GJ, Paizao VB, et al. [2017] *Neuron* 95:1171–1180. With permission from Elsevier Inc. D & E, from Markowitz JE, Gillis WF, Beron CC, et al. [2018] *Cell* 174:44–58. With permission from Elsevier Inc.)

various kinds of motor system problems, such as **ataxia**, an abnormality in coordinated muscle contraction and movement. For example, transgenic mice with disrupted cerebellar connectivity cannot walk in a straight line; instead, they wobble from side to side (**Figure 8-25**). How does the cerebellum control movement? Before answering this question, we first need to examine its circuitry, which is in fact one of the best understood in the mammalian brain due to the small number of constituent cell types (**Figure 8-26**A).

The most morphologically complex neuron in the cerebellum is the **Purkinje cell** (Figure 1-11). Each Purkinje cell extends an elaborate planar dendritic tree that receives excitatory synapses from 10^4–10^5 **parallel fibers** that intersect with the Purkinje cell dendrites at right angles (Figure 8-26A). Parallel fibers are axons of **granule cells**, whose small cell bodies are densely packed in the granular layer and receive excitatory input from **mossy fibers** originating from heterogeneous populations of neurons in the pons, medulla, and spinal cord. (Remarkably, cerebellar granule cells are so numerous that they account for more than half of all

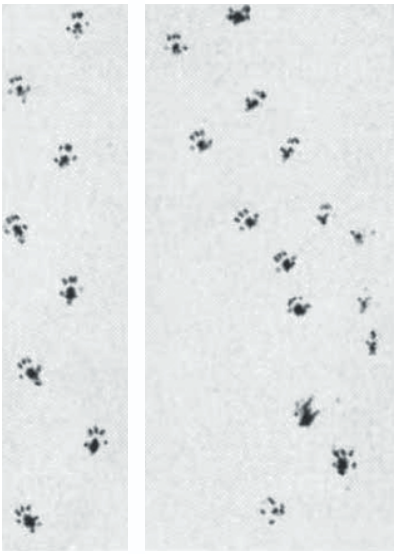

Figure 8-25 Ataxia caused by a cerebellar defect. The hind feet of mice were dipped in paint and their footprints recorded on paper. Compared with normal mice, which walk straight, mice with cerebellar defects—in this case due to connection abnormalities of Purkinje cells—typically wobble from side to side, with inconsistent step sizes and more widely spaced hind feet. (From Luo L, Hensch TK, Ackerman L, et al. [1996] *Nature* 379:837–840. With permission from Springer Nature.)

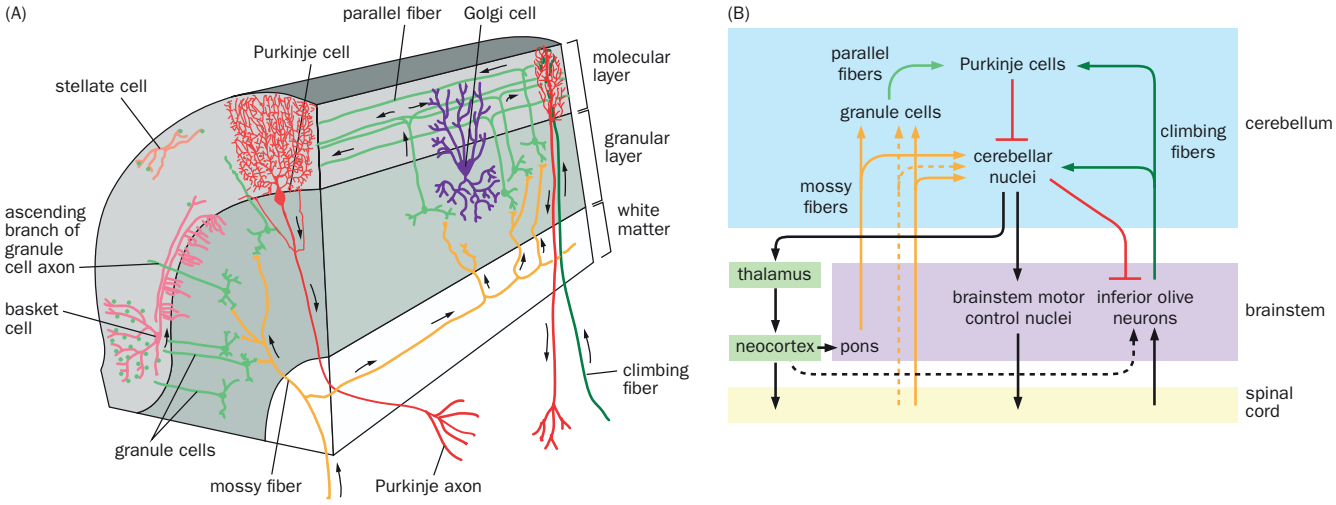

Figure 8-26 Organization of cerebellar circuitry. (A) Organization of the cerebellar cortex. Purkinje cell bodies form a single layer between the molecular and granular layers and send output to the cerebellar nuclei via the white matter. Their planar dendrites extend across the entire depth of the molecular layer. Granule cells are located in the granular layer. Their axons first ascend into the molecular layer, then bifurcate to form parallel fibers that span up to 2 mm (green dots in the cross section), each intersecting with hundreds of Purkinje cell dendrites. Two external inputs, mossy fibers and climbing fibers, synapse onto granule cells and Purkinje cells, respectively. Also drawn are the basket, stellate, and Golgi cells, three major types of local GABAergic neurons. Arrows indicate the flow of information. **(B)** Schematic summary of major connections within the cerebellum and between the cerebellum and other brain regions involved in motor control. Cerebellar granule cells receive input from mossy fibers originating from the pons, which receives descending input from the neocortex, and, directly (solid arrow) or indirectly (dotted arrow), from the spinal cord. Inferior olive neurons send climbing fibers to Purkinje cells. The cerebellar nuclei, which receive input from Purkinje cells and collaterals of mossy fibers and climbing fibers, send excitatory output to brainstem nuclei involved in motor control and to the neocortex via the thalamus. The cerebellar nuclei also send inhibitory output to the inferior olive neurons, which also receive input from the spinal cord and (indirectly) from neocortex. Note that this diagram focuses mostly on spinal cord–based motor control; input and output may vary in other systems; see Figure 8-28 for an example in vestibular control of eye movement.

neurons in the mammalian brain.) Each Purkinje cell is also innervated by just *one* **climbing fiber**, an axon originating from a neuron in the **inferior olive** nucleus in the caudal brainstem (Figure 8-19C) that "climbs" the major branches of the Purkinje cell's dendritic tree, forming numerous excitatory synapses along the way. Purkinje cells are GABAergic and send inhibitory signals to neurons in the **cerebellar nuclei**, the output nuclei of the cerebellum. Major projection targets of the cerebellar nuclei include the brainstem motor nuclei for descending motor control and the thalamus for communication with the neocortex. Both mossy fibers and climbing fibers also send collateral branches directly to the cerebellar nuclei (Figure 8-26B).

In addition to these projection neurons, the cerebellar cortex also contains three major types of local interneurons—the **basket cell** (Figure 1-15B), **stellate cell**, and **Golgi cell** (Figure 8-26A). All three cell types receive input from parallel fibers in the molecular layer. Basket and stellate cells send inhibitory output to Purkinje cells at their somata and distal dendrites, respectively, thus executing feedforward inhibition. Golgi cells send inhibitory output back onto granule cells, thus executing feedback inhibition (Box 1-2).

This circuit organization is repeated across the entire cerebellum, making the cerebellum a crystalline-like structure. The cerebellar cortex has a coarse somatotopic map. For instance, the medial and lateral parts of the cerebellum preferentially regulate trunk and limb movement, respectively. They also preferentially receive mossy fiber inputs from the spinal cord (in some cases via intermediate brainstem nuclei) and from the cerebral cortex (via the intermediate **pontine nuclei** located in the basal pons), respectively. However, such divisions are by no means absolute (see Figure 8-27A). Finally, Purkinje cells from the most posterior part of the cerebellum, the flocculus, directly innervate the vestibular nuclei instead of the cerebellar nuclei; the flocculus receives mossy fiber input preferentially from the vestibular nuclei in return (see Figure 8-28).

8.11 The cerebellum refines motor execution through feedback and feedforward regulations

How does the cerebellum regulate motor function? Shortly after the circuit architecture of the cerebellar cortex was delineated, David Marr and James Albus proposed a theory of cerebellar function around 1970 that is still influential today. The first element of the theory relates to the possible computational function of the numerous granule cells. As discussed in the previous section, 10^4–10^5 granule cells innervate each Purkinje cell. On the other hand, each granule cell receives just four mossy fiber inputs, one at each of its four dendritic claws (**Figure 8-27**A). It was proposed that the large number of granule cells enables random recombination of mossy fiber inputs, representing disparate information (related to, for example, motor commands, motor execution, or sensory feedback in the context of motor control), and hence create a high-dimensional representation of inputs. In other words, information encoded by mossy fibers is re-encoded by granule cells in a high-dimensional space, where each axis is defined by the firing rate of a single granule cell (see Figure 6-27 for an illustration, and Section 14.31 for a general discussion of encoding). This high-dimensional re-encoding can be used to separate similar patterns that are not linearly separable in low-dimensional representations (Figure 8-27B), a concept termed **pattern separation** in theoretical neuroscience. Recent anatomical and physiological studies support the notion that individual granule cells can receive input from disparate mossy fibers (Figure 8-27A).

The second key element of the theory posits that coincident firing of the granule cells and climbing fiber innervating the same Purkinje cell would result in changes in synaptic connection strength between parallel fibers arising from those specific granule cells and the Purkinje cell. This property would allow the climbing fiber to serve as a teaching signal that would regulate the transmission of information from a granule cell population representing a specific motor program to the Purkinje cell, thereby modulating cerebellar output during that motor program. Subsequent physiological studies have indeed shown that coincident firing of the climbing fiber and parallel fibers causes a *decrease* in synaptic efficacy between the active parallel fibers and the Purkinje cell, a process called **long-term depression**, which will be discussed in more detail in Chapter 11.

Let's use an example to illustrate how the cerebellar theory applies to a specific biological process: the vestibulo-ocular reflex (VOR) we introduced in Box 6-2.

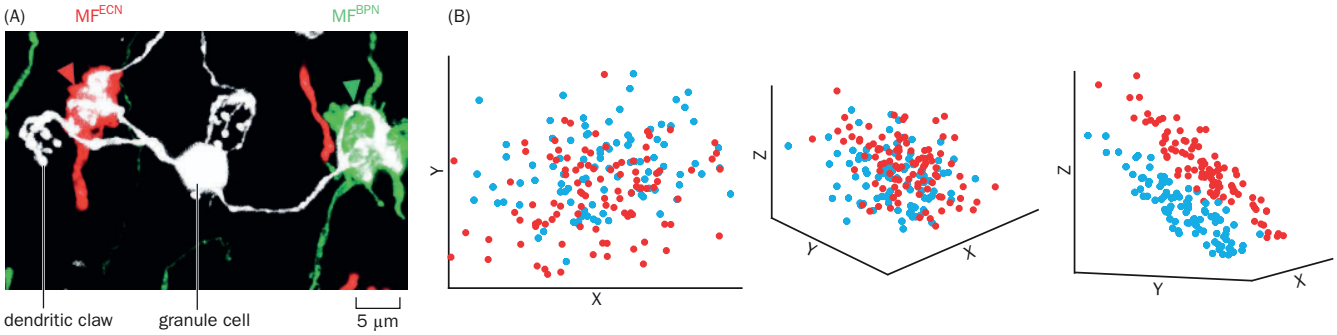

Figure 8-27 Input convergence onto granule cells and pattern separation by dimensionality expansion. (A) In this experiment, a sparse subset of granule cells (white) are labeled in a transgenic mouse, revealing dendritic claws that belong to the same granule cell. Adeno-associated viruses (AAVs) expressing green or red fluorescent proteins were injected into the external cuneate nucleus (ECN, which relays upper body proprioceptive input to the cerebellum) or basal pontine nucleus (BPN, which relays neocortical input to the cerebellum), resulting in axons (mossy fibers) labeled in green or red. The micrograph shows a single granule cell receiving convergent mossy fiber (MF) inputs from ECN and BPN onto two of its claws. **(B)** Graphs illustrating how high dimensional representations are used for pattern separation. The red and blue data points are intermingled in a two-dimensional space (left panel) and cannot be linearly separated (that is, we cannot draw a line with all the red dots on one side of it and all the blue dots on the other). However, after adding a third dimension (middle panel), the red and blue dots can be separated by a plane in three-dimensional space, as seen when rotating the axes (right). (A, from Huang CC, Sugino K, Shima Y, et al. [2013] *eLife* 2:e004000. B, courtesy of Mark Wagner. For the cerebellar theory, see Marr D [1969] *J Physiol* 202:437–470; Albus JS [1971] *Math Biosci* 10:25–61.)

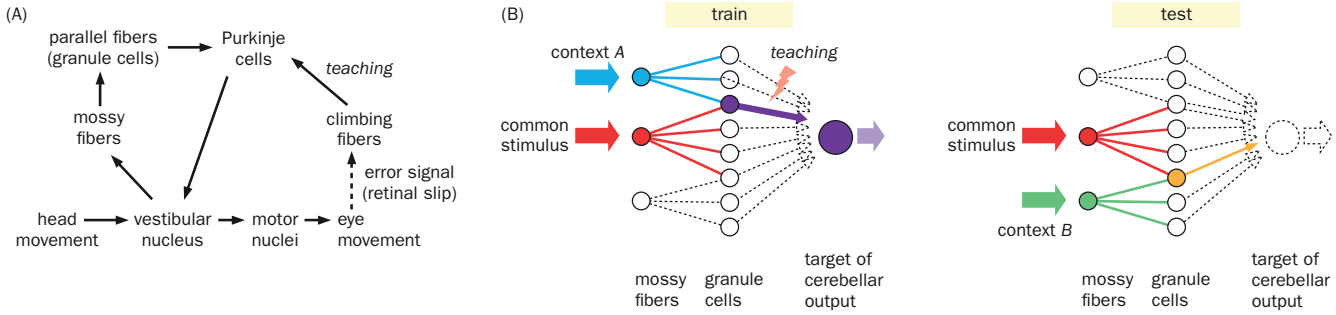

Figure 8-28 Cerebellar function in adjusting vestibulo-ocular refex (VOR) gain. (A) In the VOR, the head movement signal is relayed to the vestibular nuclei to control eye movement (bottom pathway; see Figure 6-61 for more details), but the signal strength can be adjusted by the cerebellar cortex loop detailed here. The head movement signal reaches the cerebellar cortex via mossy fibers from the vestibular nucleus, and an error signal caused by image movement on the retina (retinal slip) reaches the cerebellar cortex via climbing fibers (dashed arrow represents indirect connection). Pairing of these signals modifies parallel fiber → Purkinje cell synaptic strengths, which alters the signals sent to the vestibular nuclei, thereby adjusting VOR gain. Thus, error signals "teach" circuits through modification of synaptic strengths. **(B)** Schematic illustrating the specificity of cerebellum-based learning. Filled circles and solid lines indicate active neurons and connections. Re-encoding of mossy fiber input signals by granule cells allows learning-related circuit changes to be confined to granule cells receiving input both from a common stimulus *and* a signal representing a specific training context *A*. The thick purple arrow symbolizes strengthened cerebellar output due to learning. (While the granule cell → Purkinje cell connection is weakened by long-term depression, cerebellar output is strengthened, as Purkinje cells are GABAergic inhibitory neurons.) After training, application of the common stimulus in context *A* increases the cerebellar output, triggering target activation. When the common stimulus is presented with a distinct context *B*, however, the altered granule cell → Purkinje cell synapses are not engaged and thus the cerebellar output signal (yellow) is below the threshold to trigger target activation. (Modified after Boyden ES, Katoh A, & Raymond JL [2004] *Ann Rev Neurosci* 27:581–609; see also Ito M [1982] *Ann Rev Neurosci* 5:275–296.)

Recall that the VOR causes a compensatory eye movement in the direction opposite to a head turn, thus stabilizing visual images on the retina during head turns. However, when a change in circumstances (for example, wearing a pair of glasses that shrink the size of visual images) causes a mismatch between the magnitude of eye rotation and head turn, the VOR gain (the ratio between eye and head velocities) is adjusted by cerebellum-based motor learning. Specifically, head movement produces vestibular signals in the semicircular canals sent via mossy fibers from the vestibular nucleus to the cerebellum. An error signal resulting from retinal slip (imperfect VOR that fails to stabilize images during a head turn) is sent to the cerebellum via climbing fibers. Repeated pairings of the error signal with the vestibular signal modify the synaptic connection strength between parallel fibers and Purkinje cells, which alters the signals sent back to the vestibular nuclei, thereby adjusting the strength of VOR signals sent to motor nuclei controlling the eye movement (**Figure 8-28**A).

Experimental data also indicate that VOR gain adjustment exhibits context specificity. For instance, VOR gain learned when the head is tilted at a specific angle does not apply to situations in which the head is tilted at a different angle, and VOR gain learned during low-speed head rotation does not apply to high-speed head rotation. How does such specificity arise? Here is where the large number of granule cells and high dimensionality come into play. Suppose that one mossy fiber input represents a common left-turning-head stimulus (which causes eyes to turn right via the VOR), and other mossy fibers represent specific contexts, such as angles of head tilt or speeds of head rotation. The large number of granule cells enables the common stimulus to be recombined with specific contexts in different granule cells (Figure 8-28B). Suppose further that granule cells are activated only by simultaneous activation of more than one mossy fiber. Then the teaching signal from the climbing fiber would adjust the synaptic strength only between the granule cell carrying the common stimulus *and* the signal representing specific context during training, and thus VOR gain is altered only in that specific context. Thus, the combination of two properties—re-encoding of mossy fiber input by granule cell populations and modification of connection strengths between specific granule cells and Purkinje cells—can in principle account not only for adjustment of VOR gain but also for its context specificity (Figure 8-28B).

These theoretical predictions have largely been supported by experimental data; however, evidence suggests that VOR gain adjustment is additionally influenced by changes in input–output connectivity within the vestibular nucleus instructed by signals from the cerebellum. In addition, recent studies indicate that granule cell re-encoding of mossy fibers may not generally apply; for instance, simultaneous imaging of motor cortical output and granule cells revealed that motor learning causes granule cells to faithfully transmit cortical inputs rather than extensively re-encode such inputs.

In addition to receiving *feedback* signals from sensory systems (such as retinal slip in the VOR example), the cerebellum also receives abundant *feedforward* signals from motor systems. In the context of spinal cord–mediated movement, for example, mossy fibers carry at least three types of signals: (1) signals related to motor performance (feedback from proprioceptive sensory neurons), (2) signals related to motor intent (output signals from premotor and motor neurons), and (3) signals related to motor commands (from the motor cortex relayed through the pons). The latter two are feedforward **efference copies** of motor signals, as they are sent to the cerebellum prior to motor execution. In motor control, sensory feedback is critical for motor planning, but the actual sensory feedback is out of date by the time it reaches the brain. Efference copy signals arising from motor output pathways are thought to allow the cerebellum to construct a **forward model** of *expected* sensory feedback to provide online (real-time) tuning of motor output. If the *actual* sensory feedback (reaching the cerebellum through different routes) differs from the expected sensory feedback, the cerebellum can modify the forward model using mechanisms analogous to the VOR gain adjustment we just discussed so as to provide more accurate online tuning of motor output.

Recent evidence has indicated that the cerebellum is involved in processing cognitive and reward signals, in addition to its classic role in motor control. Indeed, across the entire neocortex, layer 5 subcerebral projecting neurons innervate the basal pons (Figure 7-32) in a topographic manner and thereby communicate with the cerebellum via just one intermediate station. In return, cerebellar nuclei project axons to much of the neocortex via the thalamus (Figure 8-26B). Thus, the cerebellum may participate in all functions carried out by the neocortex through these reciprocal loops, utilizing a common circuit motif for feedforward and feedback controls. Much remains to be learned about the functions and mechanisms of such reciprocal communication between the neocortex and cerebellum, two structures that altogether contain 99% of all neurons in the human brain.

8.12 Voluntary movement is controlled by the population activity of motor cortex neurons

In mammals, the motor cortex, which includes the **primary motor cortex** (also termed **M1**) and the more anterior **premotor cortices**, provides the ultimate command to initiate voluntary movement and control complex movements. The motor cortex integrates information from multiple sensory systems (see Section 8.13) and sends descending axons to motor control regions of the brainstem, spinal cord interneurons, and (in certain primates, including humans) motor neurons themselves (Figure 8-2). The relative contributions of these pathways to motor control are not entirely clear. Evidence suggests that M1 tends to control fine movement of distal limbs more directly and trunk muscles more indirectly via the brainstem and spinal cord interneurons. The motor cortex also communicates extensively with the basal ganglia and cerebellum to refine motor output. How these circuits act in concert to orchestrate motor control is largely unknown.

How is the motor cortex functionally organized? As discussed in Section 1.11, M1 contains a somatotopic map, the motor homunculus (Figure 1-25); this was originally discovered in nonhuman primates and in human patients undergoing neurosurgery: application of brief electrical stimulation to specific areas of the motor cortex caused specific muscles on the contralateral side of the body to twitch. (The descending motor pathway crosses the midline once such that the left motor cortex controls the right side of the body.) Depiction of the motor homunculus

Figure 8-29 Microstimulation of the motor cortex can elicit complex movements. In this example, a 500-ms microstimulation at a specific site in the arm area of M1 caused the contralateral arm to move toward the mouth regardless of its initial position. At the same time, the hand was changed to a grip posture toward the mouth, and the mouth opened, mimicking a feeding behavior. The dotted lines represent 11 different trajectories traced from video recordings at 30 frames per second. (Adapted from Graziano M, Taylor C, & Moore T [2002] *Neuron* 34:841–851. With permission from Elsevier Inc.)

gives the impression that there is point-to-point representation of muscles in M1. While regions controlling legs, trunk, arms, and face are largely segregated in the motor cortex, precise topography does not exist at a finer scale. Indeed, while brief electrical stimulation causes muscle twitching, longer stimulation can produce complex and coordinated movements, such as moving the arm toward the mouth with the hand in a grip position and opening the mouth (**Figure 8-29**). As discussed in Section 4.28, a caveat of microstimulation experiments is that the number and types of neuronal cell bodies and axons being stimulated are poorly defined. Still, the finding that specific and ethologically relevant movements can be elicited by stimulating a single site suggests that motor cortical neurons and circuits can encode motor programs for specific behaviors.

In vivo electrophysiological recordings in behaving monkeys have provided important insights into the organization of the motor cortex at the single-neuron level. For example, individual cortical neurons in the finger representation region of M1 were recorded during an experiment in which monkeys were trained to move one finger at a time. Most individual neurons were broadly tuned to the movement of multiple fingers (**Figure 8-30**A). At the same time, neurons maximally tuned to the movement of a specific finger were distributed at multiple locations, intermingled with neurons maximally tuned to the movement of other fingers (Figure 8-30B).

Given the broad tuning of individual neurons, how does the motor cortex control specific movements? We use the control of arm reaching to illustrate. In a revealing experiment, monkeys were trained to move an arm from a starting position in the center of a cube to one of the eight corners of the cube, and thus in eight directions with equal distances in three-dimensional space. The spiking activities of hundreds of individual cortical neurons in the arm area of the motor cortex were recorded one neuron at a time during each of the eight kinds of movement. Activity of most individual neurons was modulated during more than one movement direction (**Figure 8-31**A), just as neurons in the finger area were active during movement of any of several different fingers. The "preferred direction" for each neuron, as a vector in a three-dimensional space, could nevertheless be determined based on its firing rates during the eight different movements. The direction of an arm movement could not be reliably predicted from the activity of single neurons, as each neuron was broadly tuned and exhibited variable spike rates. However, a **population vector**, constructed by summing the preferred direction vectors of several hundred neurons weighted by the magnitudes of their spike rates during movements, provided an excellent estimate of the actual arm movement (Figure 8-31B). In other words, it was possible to predict the arm movement direction based on the *population activity* of motor cortex neurons. Remark-

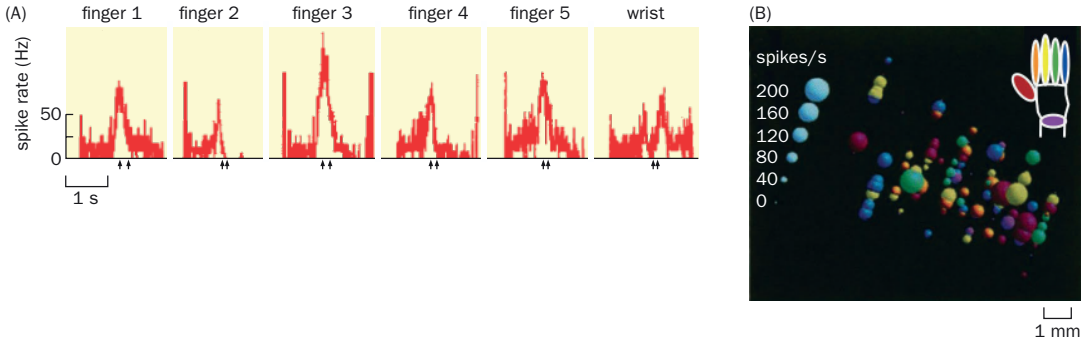

Figure 8-30 Representation of fnger mo vement in the primary motor cortex of the monkey. (A) Activity of an individual motor cortex neuron during instructed movement of five fingers and the wrist, as determined by *in vivo* extracellular recordings. The first and second arrows beneath the plot signify the beginning and end, respectively, of each movement. The cell being recorded is maximally tuned to movement of finger 3, but is active during other movements as well. **(B)** Spatial distribution of active neurons in the hand area of M1. Each neuron is color-coded according to which of the fingers (or the wrist) elicited the maximal response, following the color scheme at top right. The size of the sphere represents the spike rate notated in the key on the left. Recorded neurons form parallel lines in the same direction as that of electrode paths, from top right to bottom left. Neurons tuned to movement of the same finger(s) do not cluster at this scale. (Adapted from Schieber MH & Hibbard LS [1993] *Science* 261:489–492.)

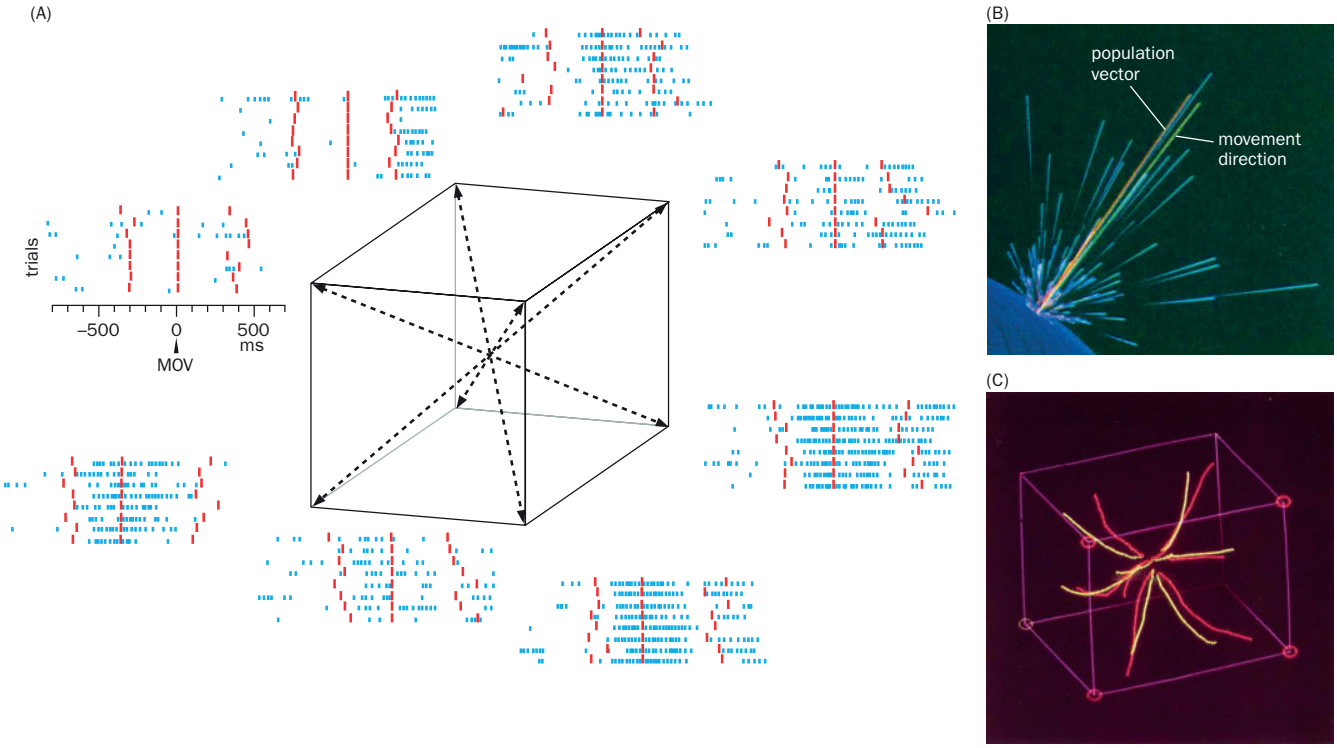

Figure 8-31 The population activity of motor cortex neurons determines movement directions. (A) A monkey was trained to move its arm from the starting position at the center of the cube to one of its eight corners upon the onset of a visual cue. The eight plots shown here illustrate spikes fired by a single neuron during each of the eight directions of arm movement. Within a plot, each row presents this neuron's spiking pattern during one trial. Each blue vertical bar represents a spike. The red vertical bars in the middle, which are used to align the plots, indicate the movement onset (MOV) and are labeled as $t = 0$ ms (milliseconds) in the time scale beneath the upper left plot. The red vertical bars to the left and right represent the onset of a visual cue (instructing the monkey to initiate movement) and the end of arm movement, respectively. The firing rate of this neuron changed most before and during arm movements toward the two corners at bottom right, but also when the arm moved in other directions. **(B)** The spike rates of individual neurons are represented as the lengths of individual vectors (blue) pointed in each neuron's preferred direction. The direction of the population vector of 224 individual neurons (orange, a weighted sum of individual vectors representing individual neurons) approximates the direction of arm movement (green). **(C)** The neural representations of trajectories (yellow; constructed based on each population vector over time) resemble the actual trajectories (red). (A & B, from Georgopoulos AP, Schwartz AB, & Kettner RE [1986] *Science* 233: 1416–1419. With permission from AAAS. C, from Georgopoulos AP, Kettner RE, & Schwartz AB [1988] *J Neurosci* 8:2928–2937. With permission from The Society for Neuroscience.)

ably, even the trajectory of arm movement from the reception of the start cue to the end of the movement could be approximated from time-varying spike rates of the motor cortex neuronal population (Figure 8-31C). These experiments provided strong evidence that movement direction is determined by the population activity of motor cortex neurons.

What drives activity in the motor cortex? Two major sources of cortical input to M1 are the parietal lobe, which relays integrated sensory information, and the frontal lobe, including the premotor cortex, which receives convergent input from much of the rest of the cortex and directs motor planning and volitional control of motor action. We discuss these two topics in the next two sections.

8.13 The posterior parietal cortex regulates sensorimotor transformations

The motor system often responds to sensory stimuli in a process called **sensorimotor transformation**. Returning to locomotion, if a cat sees an obstacle in its path, it must modify its stepping cycle to bypass the obstacle. Likewise, "simple" acts in our daily lives, such as catching a ball or reaching for a glass of water, require integration of the motor system with the visual system (to see the ball or the glass) and proprioceptive somatosensory system (to know where the hand is with respect to the ball or the glass). Interactions between motor and sensory systems can occur at

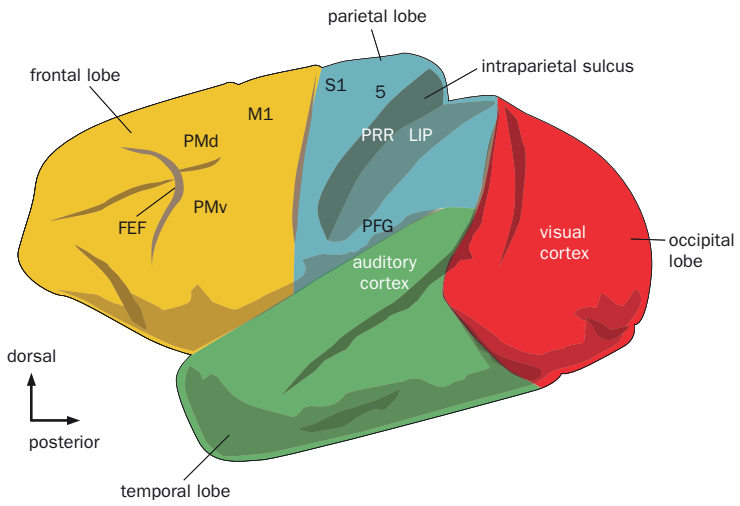

Figure 8-32 Lateral view of the monkey neocortex. Colors represent the four cortical lobes. Regions discussed in the next two sections are highlighted. The intraparietal sulcus (blue) is opened to reveal the cortical areas within the fold. FEF, frontal eye field; PMd, dorsal premotor area; PMv, ventral premotor area; M1, primary motor cortex; S1, primary somatosensory cortex; PRR, parietal reach region; LIP, lateral intraparietal area; PFG, a parietal area between PF and PG. Note that the visual cortex includes areas beyond the occipital lobe, whereas the auditory cortex occupies just a small fraction of the temporal lobe.

multiple levels. For example, proprioceptive neurons can communicate directly with motor neurons or via spinal interneurons in reflex circuits (Figure 1-19), or through many other intermediates (Figure 8-2). In this section, we study sensorimotor transformation at the level of the neocortex in the monkey (**Figure 8-32**), continuing a discussion we left off in sensory systems (Sections 4.28 and 6.35), with a focus on arm reaching.

The posterior parietal cortex, situated between the somatosensory, visual, and auditory cortices (Figure 8-32), receives input from these sensory systems and mediates multisensory integration; individual neurons often respond to stimuli of multiple sensory modalities. Interestingly, activity of posterior parietal neurons can also predict motor actions. For example, as we learned in Section 4.28, neurons in the **lateral intraparietal area** (**LIP**) can predict the direction of a saccade after integrating input from motion direction–sensitive neurons in the middle temporal (MT) visual area of the dorsal visual stream. A distinct region of posterior parietal cortex called the **parietal reach region** (**PRR**; Figure 8-32) is preferentially associated with monkeys' arm reaching: PRR neurons are activated by visual as well as proprioceptive stimuli, and in turn, their activity can predict reach movements.

In a revealing experiment, monkeys were trained to move their eyes or their hand (but not both) to a briefly presented peripheral target. Whether to move the eyes or the hand was signaled by the color of the peripheral target. A *delay* was enforced between the brief target presentation and the "go" cue; if the monkey initiated eye or hand movement before the go cue, the trial aborted and the monkey could not obtain a reward (**Figure 8-33**A). Single-unit recordings in the posterior parietal cortex identified cells that were preferentially active during the delay period before saccade (Figure 8-33B, cell 1) or before reach (cell 2). This delay period activity is exceptionally interesting to neuroscientists: it is initiated by onset of the peripheral visual target, but continues until the time of the movement, long after the target disappears. Because of its long duration, delay period activity is very different from motor neuron activity, which consists of a brief burst of action potentials immediately before movement onset. Delay period activity is thought to be related to cognitive processes such as attention, working memory, and movement preparation, as we will see later.

Analyses of recording sites indicated that the cells active before saccades were enriched in the LIP, whereas cells active before reaches were mostly found in the PRR. To address a causal role for the PRR in reach, researchers injected **muscimol**, an ionotropic GABA receptor agonist (Box 3-2), into the PRR to transiently silence neuronal activity. When PRR neurons were inactivated while monkeys performed the task, the magnitude of reach was reduced and the magnitude of saccade was unaffected (Figure 8-33C). Together, these experiments suggest that PRR neurons encode the intent to reach and are necessary for reach precision.

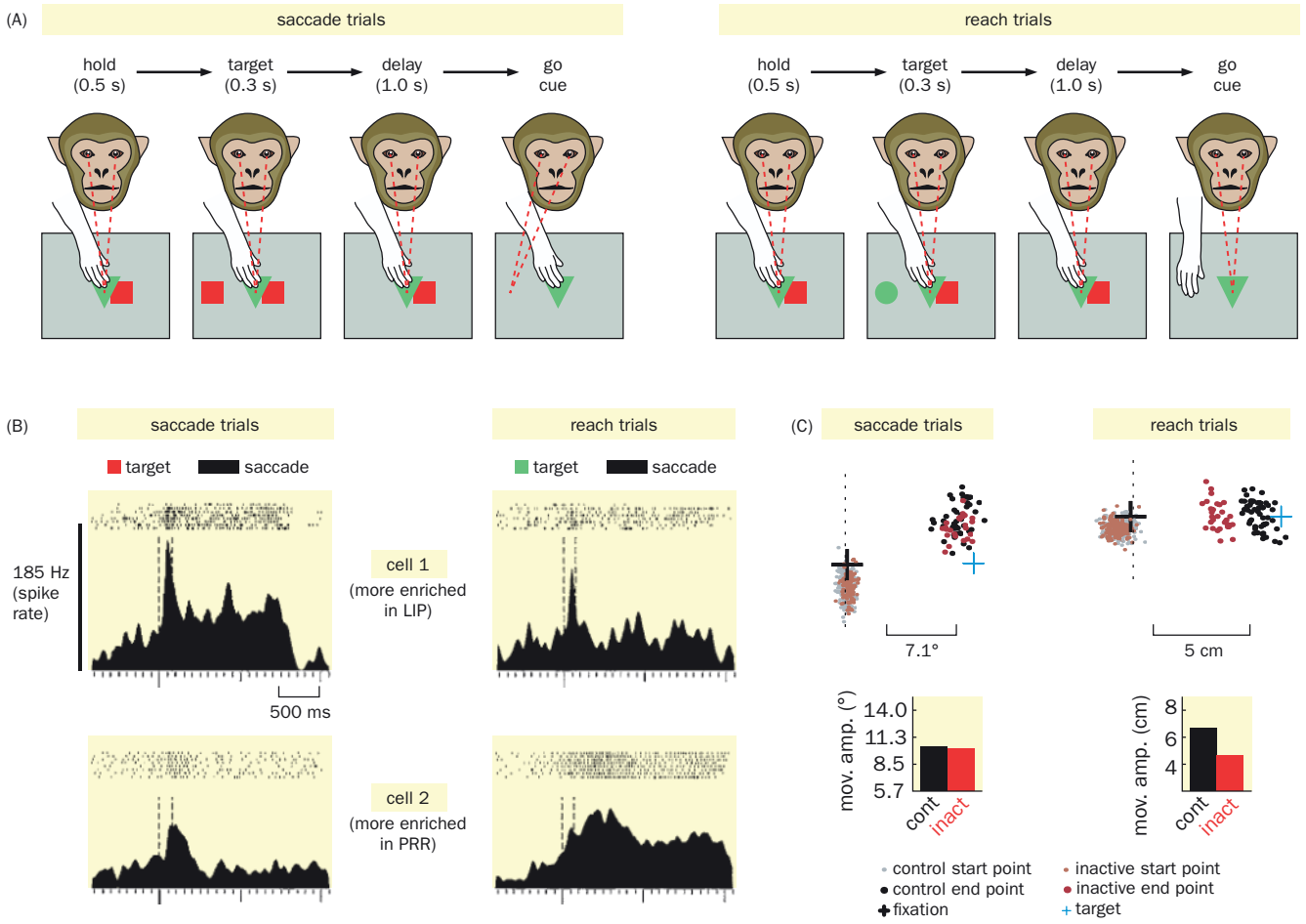

Figure 8-33 A posterior parietal cortex region involved in hand reaching. (A) Task structure. The monkey is trained to fix its eyes and place its hand at the center of the screen at the beginning of a trial. The red square and green triangles at the center are targets for eye and hand fixation, respectively. A new target transiently appears on the side, with a red square indicating a saccade trial (left) and a green circle indicating a reach trial (right). After the go cue (the disappearance of the central target for eye or hand fixation), the monkey either makes a saccade or a hand reach toward the area of the transient target. **(B)** Single-unit recordings of two representative cells in the posterior parietal cortex during saccade (left) or reach (right) trials. Each row at the top shows every third spike recorded during each of the eight trials, and the bottom shows the corresponding peri-event time histogram. Both cells increase their spike rates transiently to target stimuli. The firing rate of cell 1 is elevated above baseline during the delay period leading to saccades, whereas the firing rate of cell 2 increases during the delay period leading to reaches. **(C)** Behavioral effect of silencing PRR neurons by local infusion of muscimol. Top, data from individual trials (each dot represents one trial). Bottom, average data for eye or hand movement. Compared to control, muscimol infusion does not affect saccades (left) but reduces the magnitude of reaches (right). (A & C from Hwang EJ, Hauschild M, Wilke M, et al. [2012] *Neuron* 76:1021–1029. With permission from Elsevier Inc. B, adapted from Snyder LH, Batista AP, & Andersen RA [1997] *Nature* 386:167–170. With permission from Springer Nature.)

Sensorimotor transformation is more than simply relaying information between the sensory and motor systems. In visually guided reaching, for example, sensory information arrives in eye-centered coordinates, whereas motor output is produced in hand-centered coordinates (**Figure 8-34**). Single-unit recordings indicated that PRR neurons encode target location in eye-centered coordinates, whereas neurons in Area 5 of the posterior parietal cortex (Figure 8-32) encode target location in both eye- and hand-centered coordinates. In principle, hand-centered coordinates can be derived by subtracting hand location from target location in eye-centered coordinates (Figure 8-34), and neurons in Area 5 may represent an intermediate step in this transformation.

The posterior parietal cortex is also involved in online monitoring and correction of movement trajectories. As discussed in Section 8.11, effective online control requires a *forward model* using efference copy signals to estimate the upcoming states of the movement rather than relying solely on visual or somatosensory feedback, which have delays of 30–90 ms. Analyses of movement angle

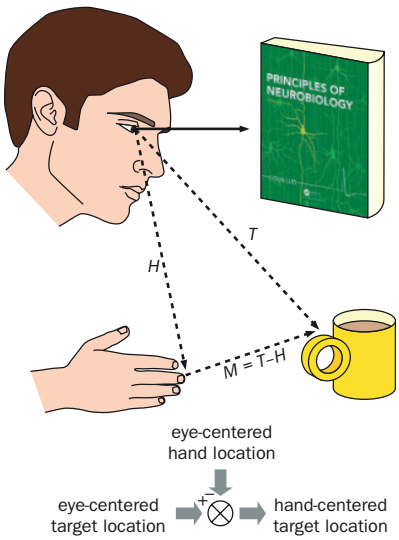

Figure 8-34 Transforming eye-centered coordinates into hand-centered coordinates in visually guided reaching. Top, schematic illustrating the target (coffee mug) and hand in eye-centered coordinates (vector *T* and *H*, respectively) and target in hand-centered coordinates (vector *M*). Bottom, illustration of the transformation from eye-centered target location to hand-centered target location. (From Buneo CA, Jarvis MR, Batista AP, et al. [2002] *Nature* 416:632–636. With permission from Springer Nature.)

encoding during reaching revealed that while some posterior parietal cortical neurons had lag times of 30–90 ms, consistent with their receiving sensory feedback, the majority of neurons had shorter or no lag times, supporting their participation in forward models. Taken together, these experiments suggest a key role for the posterior parietal cortex in sensorimotor transformation during visually guided reaching. Indeed, human patients with strokes affecting the posterior parietal cortex suffer from **optic ataxia**, an inability to guide the hand toward an object using visual information, even though other aspects of their movement and vision are less affected.

8.14 The frontal cortex regulates movement planning: a dynamical systems perspective

In addition to the parietal cortex, the frontal lobe anterior to the primary motor cortex houses many neurons whose activity, referred to as **preparatory activity**, precedes the onset of motor commands. For example, neurons in the dorsal premotor cortex (PMd; Figure 8-32) are well known to exhibit preparatory activity prior to arm-reach movement. Preparatory activity is most common in tasks involving an enforced delay before a go cue for movement initiation (Figure 8-33), but similar preparatory activity can also be found following sensory cues but before movement even without an enforced delay. Preparatory activity in premotor cortex is specific to the upcoming movement, can reduce reaction time and increase accuracy compared to movement without a preparatory period, and when disrupted, can delay movement onset. Thus, preparatory activity in premotor cortex plays an important role in movement planning.

Because many premotor cortex neurons are also active during the actual movement, and indeed some also send descending axons to the spinal cord, a question arises as to why preparatory activity does not lead to movement. Before addressing this question, we introduce a new perspective on how motor action is represented by activity of neuronal populations. As discussed in Section 8.12, *in vivo* recordings indicate that activity of most motor cortex neurons correlates with contraction of specific muscles as well as specific movement parameters such as direction, magnitude, and velocity. This phenomenon, known as multiple selectivity (individual neurons can encode multiple signals in their activity), raises the intriguing question of how downstream circuits decode specific signals in order to generate motor behavior. Instead of asking this question from the perspective of individual neurons, an alternative perspective on motor control treats the motor cortex as a **dynamical system**, composed of different **dynamical states** that evolve over time according to specific rules. Recall that in our discussion of olfactory coding, we introduced the concept that the activity state of a neuronal population can be represented as a point in a multidimensional space, with each axis representing the firing rate of one constituent neuron (Figure 6-28A). Likewise, the dynamical state of the motor cortex at any given time can be described as the firing rates of a population of motor cortex neurons at that time. The activity of motor cortex neurons over time can be represented as an evolving dynamical state that follows a specific trajectory in the activity state space (**Figure 8-35**A).

We use a specific example to illustrate how the dynamical systems perspective provides insight into cortical control of movement. In a reaching task, a monkey was trained to move its arm toward a target on the screen, but only after a go cue appeared (Figure 8-35B, top). Trajectories of neural states throughout each of many individual trials were computed from activity of hundreds of *simultaneously* recorded dorsal premotor cortex neurons (Figure 8-35B, bottom) using a **multielectrode array** (see Figure 14-36 for details). Target appearance caused the starting positions of different trials, which were initially more variable (blue ellipse), to converge onto a smaller region in the state space during movement preparation (green ellipse). The onset of the go cue caused the neural states to move into yet another small region at the time of movement onset (gray ellipse), following similar trajectories across different trials. These observations suggest that stimulus onset reduces the variability of population activity of the premotor cortex.

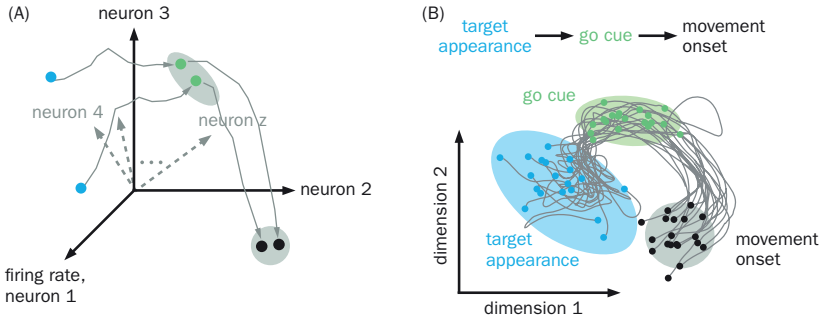

Figure 8-35 A dynamical systems perspective on motor control. (A) The dynamical state of the motor cortex at a given time is a vector in a high-dimensional activity state space, with values on each axis representing the firing rates of individual neurons. The first three dimensions are shown here as solid arrows, and other dimensions are symbolized by dashed gray arrows in the background. Time is implicit in this diagram; the passage of time is represented by a trajectory in the state space. Two example trajectories representing two trials of the behavioral task in Panel B are schematized. **(B)** Top, behavioral task. The monkey is trained to move its arm to reach a target shown on a screen only after a subsequent go cue appears. Bottom, motor cortex activity for 18 different trials, represented by 18 trajectories in the state space. Blue, green, and black circles represent neural states (computed from activity of hundreds of simultaneously recorded cortical neurons) just before target appearance, at the appearance of the go cue, and at movement onset, respectively. Trajectories between blue and green circles represent movement planning, while trajectories between green and black circles represent movement initiation. The high-dimensional state space in Panel A is simplified by projecting it onto two dimensions while preserving the relative size of the ellipsoids representing variance across trials. (Adapted from Shenoy KV, Sahani M, & Churchland MM [2013] *Ann Rev Neurosci* 36:337–359. See also Churchland MM, Yu BM, Cunningham JP, et al. [2010] *Nat Neurosci* 13:369–378.)

Having introduced the dynamical systems perspective, we now return to the question of why preparatory activity in the premotor cortex does not lead to movement. Let's begin with a simple system: a muscle receiving input from two neurons and producing a response according to the sum of their firing rates (**Figure 8-36A**). Each neuron can vary its firing rate, but if the sum of its firing rates remains the same (gray trajectories along the blue line in Figure 8-36B), no change in muscle contraction results. The blue line represents the "output-null" dimension because firing rate changes along this dimension do not cause movement. However, when additional inputs to the system cause the gray trajectories to move away from the blue line, the changes in the net output of the two-neuron system cause movement to occur by contracting or relaxing the muscle. Thus, the dimension orthogonal to the blue line (the green line) is the "output-potent" dimension in this simple two-dimensional state space.

Figure 8-36 features only two neurons, but it is easy to imagine systems of 10 or 1000 neurons in the motor cortex, where the same principles hold. As long as the sum of neural firing rates remains constant, no net motor output is transmitted to the spinal cord. Within the constraint of net equality, the activity of individual

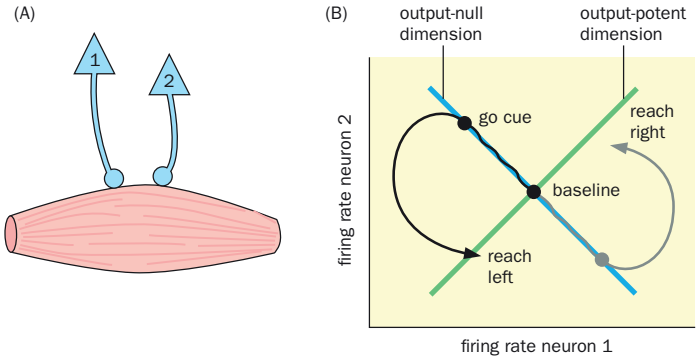

Figure 8-36 Preparatory activity resides in an output-null dimension. (A) In this two-neuron system, the muscle responds to the sum of the firing rates of neurons 1 and 2. **(B)** When changes in the activity state occur along the blue line of the two-neuron system, the sum of the firing rates for neurons 1 and 2 remains constant, and no movement results. When changes in the activity state deviate from the blue line, movement ensues. Thus, the blue line represents the output-null dimension, while the orthogonal green line represents the output-potent dimension. Drawn in two different shades of gray are two trajectories representing movement planning (when the trajectories coincide with the blue line) and movement execution (after the go cue represented by circles at the upper left and lower right), obtained from simultaneous multielectrode recordings in a task similar to that described in Figure 8-35. The two trajectories represent neural activity state changes for reach left and reach right, respectively. (Adapted from Kaufman MT, Churchland MM, Ryu SI, et al. [2014] *Nat Neurosci* 17:440–448. With permission from Springer Nature. See also Elsayed GF, Lara AH, Kaufman MT, et al. [2016] *Nat Comm* 7:13239.)

neurons in the system can move up and down, implementing computations that prepare the system for efficient movement to the correct target when the go signal is given (Figure 8-36B, upper left and lower right gray circles). This separation of output-null and output-potent dimensions in the neural activity space provides an elegant mathematical explanation for the separation of movement planning and movement execution in the same neuronal population, despite the fact that many neurons encode multiple signals in their activity (as discussed earlier). Recent multielectrode array recordings indicate that this principle is indeed implemented within premotor circuitry. The mechanisms by which population activity is restricted to the output-null dimension during movement planning and is converted to the output-potent dimension just before movement onset are unknown.

We have discussed the parietal cortex's involvement in sensorimotor transformation in Section 8.13 and the premotor frontal cortex's involvement in movement planning in this section, but these two processes are highly intertwined. Indeed, neurons in the parietal and frontal cortices communicate extensively with each other during sensorimotor transformation and movement planning and also communicate extensively with M1 during movement execution. For instance, the PRR and PMd have strong reciprocal connections that control arm reaching, while the LIP reciprocally connects with the **frontal eye field**, a premotor cortical region that controls eye movement (Figure 8-32; see also Figure 4-51). Premotor and primary motor cortical inputs to the parietal cortex provide efference copies of motor plans that help construct the forward models discussed earlier. Thus, the frontal, parietal, and primary motor cortices can be conceptualized as a giant dynamical system that underlies sensorimotor transformation, movement planning, and movement execution. Recent advances in neural circuit dissection tools in rodents have enabled more precise perturbations of neuronal dynamics, allowing examination of the causal role of preparatory activity in linking sensation to action (**Box 8-2**).

Interestingly, certain neurons in the rostral part of the ventral premotor cortex and the reciprocally connected PFG area of the posterior parietal cortex (Figure 8-32) are active not only when a monkey performs an action, such as reaching or grasping an object, but also when another monkey or a human performs the same action. These neurons are aptly named **mirror neurons**. The properties of mirror neurons have been proposed to enable monkeys to understand intention and imitate the actions of others using the framework of the monkey's own action planning. fMRI imaging studies suggest that a similar mirror neuron system is also present in the analogous regions of the human frontal and parietal cortices. The mirror neuron system provides a fascinating window into the interface between perception and action as well as the neural basis of learning by imitation.

Box 8-2 Probing the causal function of preparatory activity

Cortical control of movement planning and execution has historically been studied in nonhuman primates. Analogous investigations have recently been carried out in rodents, taking advantage of modern circuit dissection tools that are widely used in mice and rats (see Chapter 14). Here we discuss two examples of investigations into the role of preparatory activity in linking sensation to action.

In our first example, thirsty rats use the frequency of auditory stimuli to decide in which direction to orient their head to obtain a water reward (**Figure 8-37**A). A delay was enforced such that rats needed to wait until the go cue before initiating the movement. Rats can perform the task fairly well when the click frequency deviates substantially from a threshold (Figure 8-37B, solid line). When muscimol was infused into a frontal lobe premotor area called the frontal orienting field (FOF) to silence neuronal activity, rats exhibited a marked deficit in orienting toward the side contralateral to the site of muscimol infusion (Figure 8-37B, dashed line). Single-unit recordings revealed that a large fraction of FOF neurons exhibited preparatory activity during the delay period that predicted subsequent orienting direction (Figure 8-37C). Furthermore, optogenetic silencing of halorhodopsin-expressing FOF neurons (Section 14.25) during the delay period disrupted contralateral orienting, like muscimol infusion. The temporal precision of optogenetic silencing allowed researchers to conclude that preparatory activity in one side of the FOF during the delay period plays a causal role in promoting orienting to the contralateral side.

Box 8-2: continued

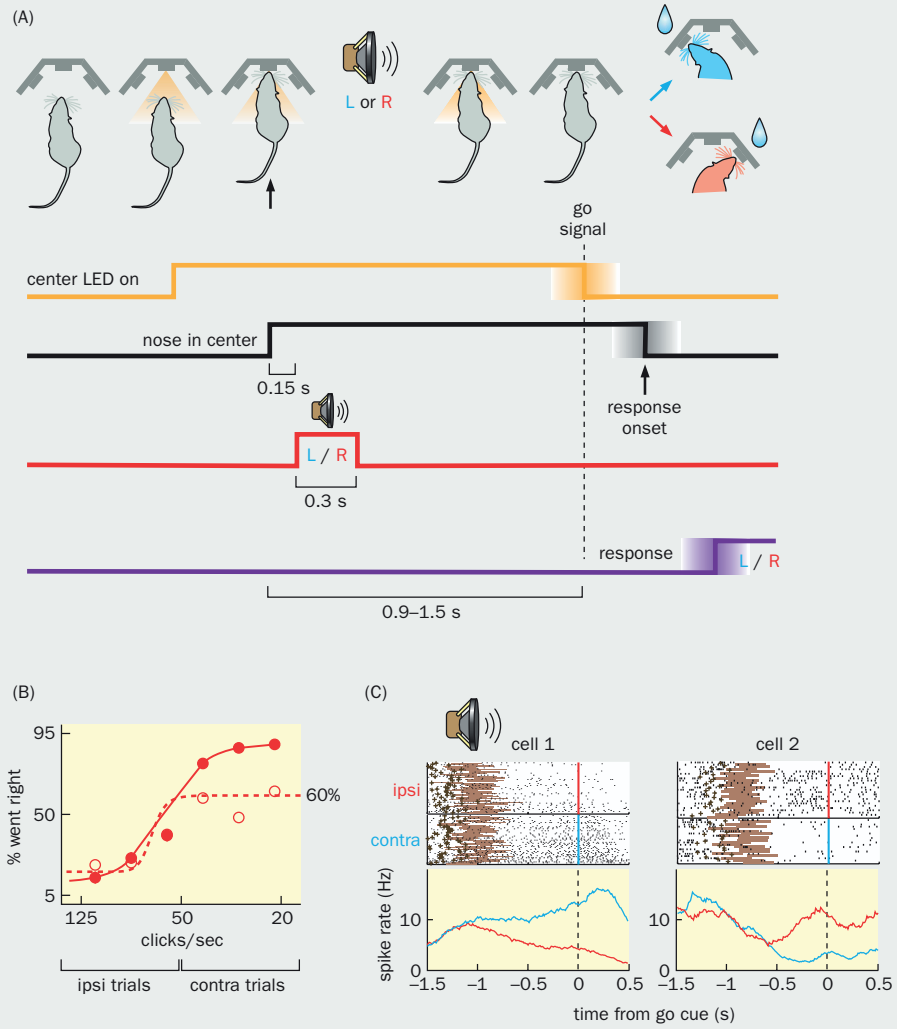

Figure 8-37 Preparatory activity in the rat frontal orienting feld (FOF) prior to orienting. (A) Task structure. Water-restricted rats were trained to poke their nose into the center port upon LED light onset. This triggers a click tone with a specific frequency; a water reward is available at the left or right port if the frequency is >50 Hz or <50 Hz, respectively. A variable delay was introduced by requiring the rat to wait until after the LED turns off (the go cue) to orient its head toward a water port to earn its reward. **(B)** Psychometric curves for normal rats (solid curve) and rats with the left FOF infused with muscimol (dashed curve). Compared with normal rats, muscimol-infused rats perform poorly in orienting to the contralateral port. **(C)** Single-unit recordings from two representative FOF cells. Top, each row shows spike patterns during one trial. Trials are aligned to the go cue (t = 0), and ipsi- and contralateral orienting trials are grouped separately. Tone periods are highlighted in brown. +, center poke onset. Bottom, peri-event time histograms of ipsi- and contralateral trials. Cell 1 exhibits more preparatory activity during contralateral trials, and cell 2 during ipsilateral trials. (From Erlich JC, Bialek M, & Brody CD [2011] *Neuron* 72:330–343. With permission from Elsevier Inc. See also Kopec CD, Erlich JC, Brunton BW, et al. [2015] *Neuron* 88:367–377.)

In our second example, head-fixed mice were trained to lick water from a left or right port depending on the position of the pole sensed by their whiskers, again after an enforced delay (**Figure 8-38**A). Researchers could silence the output of a given cortical area with high temporal precision by photostimulating transgenic mice expressing channelrhodopsin (ChR2; Section 14.25) in all GABAergic inhibitory neurons (Figure 8-38B; this is because the vast majority of GABAergic inhibitory neurons project locally, and therefore their activation silences nearby pyramidal neurons that send output from the photostimulated region to distant targets). This enabled researchers to examine the behavioral consequence of silencing different cortical areas during specific periods of the trial. For example, silencing of the barrel cortex (primary somatosensory cortical region representing whiskers; Box 5-3) during *the sample period* markedly reduced performance, validating an essential sensory function for the barrel cortex in the task. Researchers then screened for cortical areas that, when silenced during *the delay period*, would disrupt task performance. They found that a premotor area called the anterior lateral motor cortex (ALM) had the largest effect: mice displayed a marked

(*Continued*)

Box 8-2: continued

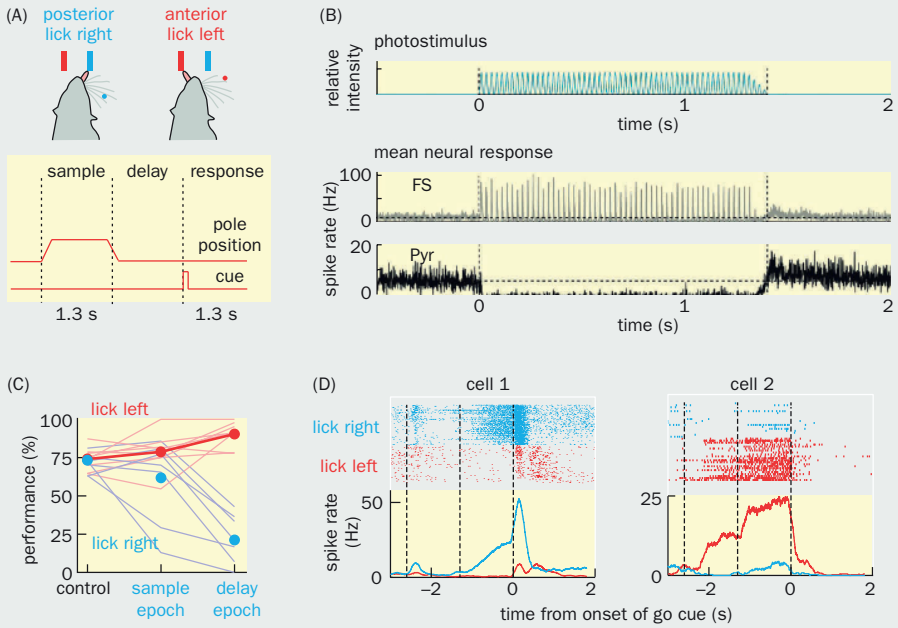

Figure 8-38 Preparatory activity in the mouse anterior lateral motor cortex (ALM) prior to licking. (A) Task structure. Water-restricted head-fixed mice were trained to respond to presentation of two vertical poles (blue and red circles) detected by their whiskers by licking the left or right water ports, as indicated. The poles were raised to the whisker level during the sample period. A delay was enforced between the end of the sample period and an auditory go cue. **(B)** Effect of silencing output of a cortical area by photostimulating inhibitory neurons using transgenic mice expressing ChR2 in all GABAergic cells. Top, photostimulation applied at 40 Hz. Middle, a neuron exhibiting fast spiking (FS), a signature of cortical GABAergic basket cells, fires action potentials time locked to photostimulation. Bottom, photostimulation of inhibitory cells silences the firing of a pyramidal (Pyr) neuron. **(C)** Effects on lick performance when the left ALM was silenced during the sample or delay epochs. Silencing the ALM during the delay epoch drastically reduced contralateral licking and slightly increased ipsilateral licking. Thin lines represent the performances of individual mice, and thick lines their averages. **(D)** Single-unit recordings from two cells, as in Panel C. Cell 1 exhibits stronger preparatory activity for licking right, and cell 2 for licking left. (A, C, & D from Li N, Chen TW, Guo ZV, et al. [2015] *Nature* 519:51–56. With permission from Springer Nature. B, from Guo ZV, Li N, Huber D, et al. [2014] *Neuron* 81:179–194. With permission from Elsevier Inc.)

reduction in subsequent licking to the contralateral port (Figure 8-38C). Single-unit recordings identified preparatory activity in many ALM neurons, some of which also exhibited trial-specific activity patterns during the sample period (Figure 8-38D). Together, these experiments identified a causal role of ALM preparatory activity in transforming whisker-based somatosensation into lick movements.

The temporal delay between sensory stimuli and movement onset in these perceptual discrimination tasks requires the animals to remember the sensory stimuli at the time of movement execution. Such short-term (on the order of seconds) memory during a task is referred to as **working memory**. Persistent activity of frontal cortex neurons has been hypothesized to be the physiological substrate of working memory. Thus, preparatory activity for movement planning can also be viewed as representing working memory that links sensation to action. What is the neural basis of persistent activity? Persistent activity has been hypothesized to be due to either intrinsic biophysical properties of the neurons or mutually excitatory local connections. A surprising finding from the rodent models discussed here is that persistent activity in the ALM and FOF is likely contributed by a brain-wide network.

For example, the ALM forms strong reciprocal connections with medial dorsal (MD) thalamic nucleus (**Figure 8-39**), which also exhibit preparatory activity. Optogenetic perturbation experiments indicated that the preparatory activity

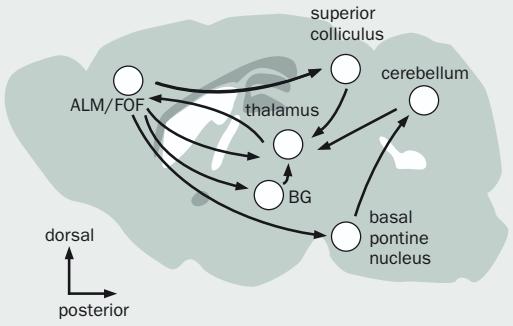

Figure 8-39 Simplifed schematic of interacting brain regions lik ely involved in maintaining persistent activity between sensation and action in a rodent brain. Arrows indicate direct projections. ALM, anterior lateral motor cortex; BG, basal ganglia; FOF, frontal orienting field. (From Svoboda K & Li N [2018] *Curr Opin Neurobiol* 49:33–41. With permission from Elsevier Inc.)

Box 8-2: continued

of the MD thalamus and the ALM mutually reinforce each other and that both are required for task performance. The ALM (and the neocortex in general) also forms bidirectional connections with the cerebellum via the basal pontine nuclei and thalamic nuclei (Figure 8-26B). Preparatory activity is also found in cerebellar neurons, and disrupting cerebellar output also interferes with preparatory activity in ALM neurons. In the orienting task described earlier, preparatory activity has also been found in the superior colliculus, a projection target of the FOF that also sends projections back to the cortex via the thalamus (Figure 8-39). Simultaneous silencing of the FOF and superior colliculus synergistically disrupted task performance (that is, more so than simply adding the effects of the individual perturbations), suggesting that the activities of the FOF and superior colliculus enhance each other through their reciprocal connections. Altogether, these studies suggest that multiple brain regions interact to sustain the preparatory activity linking sensation to action. These findings also highlight the importance of simultaneously studying multiple brain regions in order to decipher the principles of information processing during sensorimotor transformations.

8.15 Population activity of motor cortex neurons can be used to control neural prosthetic devices

Investigating how the neocortex controls movement not only helps us understand the neural basis of action but also has important clinical applications. Specifically, the ability to predict movement directions using the firing patterns of cortical neurons (Figure 8-31) has inspired intense research into brain–machine and brain–computer interfaces, or **neural prosthetic devices**. A major goal of these devices is to help patients suffering from paralysis due to spinal cord injury or motor neuron disease to regain voluntary motor control. These patients' motor cortices are still active and can presumably send commands to control body movement. Unfortunately, either the axons that deliver the commands to the spinal cord are damaged or motor neurons have degenerated, such that the brain and muscles are disconnected. A general strategy for creating neural prosthetic devices starts with extracting the activity of motor cortex neurons. The most effective approach thus far is an implanted multielectrode array that can directly record spikes of hundreds of individual neurons simultaneously. The activity of these neurons is then fed into a computer to extract movement intent, which is used to control an output device, such as a robotic arm (**Figure 8-40**A) or a computer cursor. Visual feedback to the patients can help them learn to change the firing patterns of the recorded neurons for better performance. Remarkable progress has been made in recent years in the accuracy, complexity, and speed of such neural prosthetic devices. We give two examples to illustrate these advances.

In the first example, a multielectrode array implanted in a monkey's motor cortex recorded spikes from 116 neurons (Figure 8-40B, top). A computer decoded these patterns in real time by extracting movement intent using a method similar to the discussed in Section 8.12. The movement intent was then executed by a robotic arm with five degrees of freedom: three at the shoulder, one at the elbow, and one at the hand for gripping. After training by fetching marshmallows as a reward, the monkey was able to control the extension of the robotic arm by "thinking" about the movement (Figure 8-40B, bottom). Such thinking caused the monkey to extend the robotic arm toward a marshmallow placed at different locations in three-dimensional space, grab the marshmallow, and bring it to its mouth (Figure 8-40C; **Movie 8-5**). Remarkably, these actions took only a few seconds and had a 60% success rate. This and other such examples suggest that this approach can help human patients with motor deficits regain movement control.

The second example is the first human clinical trial using neural prosthetics to enable a patient with tetraplegia to move a computer cursor via cortical control. The patient suffered a spinal cord injury three years before having a 100-electrode array surgically implanted into his motor cortex (**Figure 8-41**A). During the training period following surgery, the patient was asked to imagine moving his hand along the trajectory of a cursor on a computer screen controlled by a technician (Figure 8-41B). Population activity of motor cortex neurons recorded during the imagined movement was then used to construct an algorithm best matching the

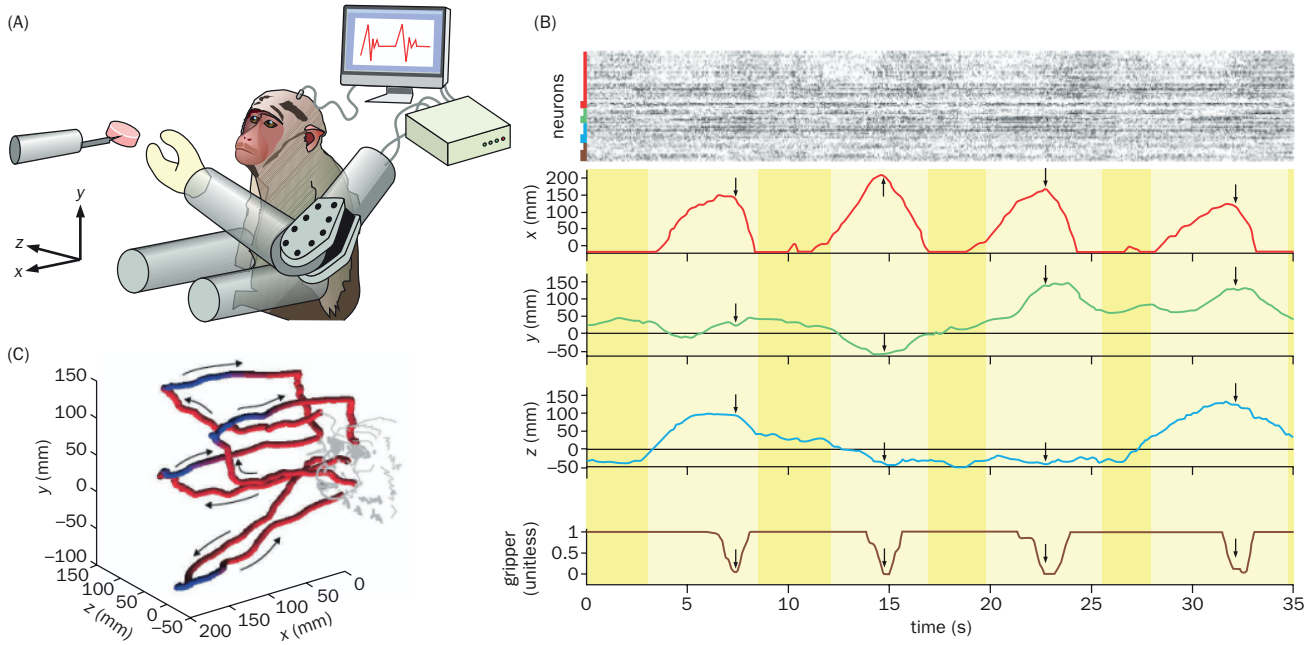

Figure 8-40 Cortical control of a prosthetic arm for self-feeding. **(A)** Schematic of a brain–machine interface for prosthetic control. A multielectrode array was implanted in the motor cortex of a monkey. The spiking patterns of many motor cortex neurons were used for real-time control of a robotic arm using a population vector algorithm (Figure 8-31). The monkey was first trained to control the robotic arm by moving a joystick with its own arm, before graduating to cortical control in this experiment, during which its own arms were restrained. **(B)** Top, spiking activity of 116 neurons used to control the robotic arm during four self-feeding trials. Each row shows a different neuron's spiking over time, with each of the four trials occurring consecutively (lighter yellow regions below). The neurons are grouped along the *y* axis based on which of the four dimensions of robot movement they responded most strongly to (red, neurons preferring motion along the *x* dimension; green, *y* dimension; blue, *z* dimension; purple, gripper movement) and also by whether they preferred movement in the negative (thin bars) or positive (thick bars) directions along that dimension. Bottom, four traces corresponding to robotic arm movement in the *x*, *y*, and *z* directions and the position of the gripper (1 = open, 0 = closed) during the four trials shown in Panel C. Arrows indicate the gripper closing on the target. **(C)** Spatial trajectories of the same four trials as in Panel B, with varied marshmallow positions. Red and blue parts of each trajectory represent open and closed grippers, respectively. Note that the monkey opened the gripper before the food reached its mouth because it learned that marshmallows tend to stick to the gripper so that it does not need to close the gripper for the full duration of the return trip. (Adapted from Velliste M, Perel S, Spalding MC, et al. [2008] *Nature* 453:1098–1101. With permission from Springer Nature.)

motor intent. During the next phase, the patient imagined moving the cursor, and the algorithm transformed his motor cortex activity, recorded from the multielectrode array, into real-time control of the computer cursor. After extensive training, the patient could perform a variety of computerized tasks, such as moving a cursor to designated targets while avoiding obstacles (Figure 8-41C), opening files in an email inbox, and drawing circles (Movie 8-5), all via imagined motion.

Despite these remarkable achievements, human clinical trials have also revealed important limitations: the speed, accuracy, and level of control are considerably less than control of a computer cursor via a standard mouse by hand. The long-

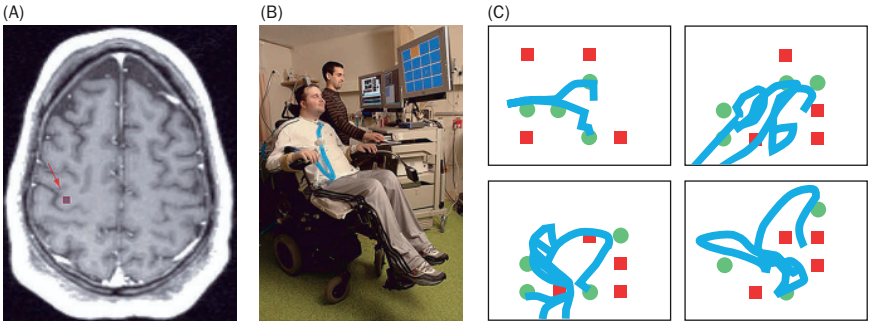

Figure 8-41 Movement control for a human tetraplegia patient via a brain-computer interface. **(A)** A magnetic resonance image of the patient's brain before surgical implantation of a 4 mm × 4 mm multielectrode array in the arm control region of the right motor cortex. The square indicated by the red arrow denotes the target position of the implant. **(B)** The computer cursor was controlled by the patient's motor cortex activity, as recorded by the multielectrode array. **(C)** Example of a cursor control task performed by the patient involving acquisition of targets (green circles) and avoidance of obstacles (red squares). Blue lines denote the cursor trajectory in four separate trials. (Adaped from Hochberg LR, Serruya MD, Friehs GM, et al. [2006] *Nature* 442:164–171. With permission from Springer Nature. See Pandarinath C, Nuyujukian P, Blabe CH, et al. [2017] *eLife* 6:e18554 for a recent example of typing with a brain–computer interface.)

term stability of electrode arrays also limits such trials. Researchers are making remarkable progress in addressing these limitations. In a recent study, for example, brain–computer interfaces enabled some patients to type with a computer keyboard at a speed of ~30 correct characters per minute (about a third to half the speed of able-bodied subjects typing on a smartphone), thus greatly facilitating their communication capabilities.

In addition to helping patients, neural prosthesis research has also provided important insights into how the motor cortex controls voluntary movements. Each motor task appears to be controlled by an ensemble of cortical neurons—this is supported by the successful extraction of spiking activity from populations of neurons to control prosthetic devices and the dependence of this success on engaging a critical number of neurons (ranging from dozens to hundreds). At the same time, each individual neuron contributes to multiple tasks—for instance, movement in all three dimensions of space and grip, as shown in the example in Figure 8-40. These properties may explain why information from several hundred neurons—a very small fraction of all motor cortex neurons—can allow remarkable control of prosthetic devices. From a dynamical systems perspective, neural states extracted from the activity of a few hundred neurons can be useful approximations of neural states of an entire subregion in the relevant motor homunculus for executing well-trained tasks. The improvement in performance by learning through visual feedback suggests that cortical neuronal ensembles that control movement are plastic—indeed, this was observed when monitoring changes in the tuning properties of individual neurons and neuronal ensembles as animals learned to improve their performance via training. We will return to the subject of learning and plasticity in Chapter 11.

SUMMARY

Motor systems are organized hierarchically. The powerful neuromuscular junction converts nearly every action potential from motor neurons into muscle contractions via rises in intracellular Ca^{2+}, which triggers sliding of actin and myosin fibers. Thus, the end goal of motor control is to specify motor neuron firing patterns. Motor neurons integrate information from multiple sources, including input from spinal premotor neurons, descending commands from brainstem motor control nuclei and the motor cortex, and sensory feedback from proprioceptive neurons. In rhythmic motor programs such as locomotion, the rhythmic output pattern is produced by central pattern generators in the spinal cord in the absence of sensory feedback and activated by brainstem motor control nuclei. The mechanisms by which central pattern generators operate are best understood in invertebrate systems, where the biophysical properties of constituent neurons and their connection patterns and strengths determine the rhythmic output patterns. Modern genetic and circuit analysis tools have begun to enable dissection of complex circuits in the spinal cord and brainstem that control various motor behaviors, from locomotion to breathing.

Voluntary movement is controlled by the motor cortex via extensive collaboration with the basal ganglia and cerebellum, both employing generic circuit designs. In the striatum of the basal ganglia, two types of spiny projection neurons both receive cortical and thalamic inputs and separately constitute the direct and indirect pathways, which control basal ganglia output. The direct and indirect pathways are bidirectionally modulated by midbrain dopamine neurons and act in concert to regulate the selection and initiation of motor programs. The cerebellum utilizes a vast number of granule cells to integrate inputs concerning motor commands from the motor cortex and brainstem, motor performance from premotor neurons in the spinal cord, and feedback from sensory systems. The cerebellum constructs a forward model that predicts the sensory consequences of movement in order to adjust motor output. The motor cortex is grossly organized in somatotopy, but this somatotopy breaks down at fine scales. While each motor cortex neuron is broadly tuned to multiple motor tasks, population activity of motor cortex neurons can be predictive of movement parameters, such as the direction

and trajectory of arm reaching. The population activity of motor cortex neurons has been used to control neural prosthetic devices with remarkable success.

The posterior parietal and premotor cortices form extensive connections with each other and with the primary motor cortex. Together, these form an extended dynamical system that plays crucial functions in sensorimotor transformation and motor planning. Recent studies have implicated additional brain regions, including the thalamus and cerebellum, in maintaining preparatory activities in the transition between sensation and action. A major future challenge is to understand how neuronal populations in different brain regions cooperate to control movement planning and execution.

OPEN QUESTIONS

- How do individual spinal motor neurons integrate distinct sources of inputs to control their firing pattern?
- What are the neural substrates for central pattern generators in the vertebrate spinal cord and brainstem?
- How do neurons in different brain regions, such as the motor cortex, cerebellum, and basal ganglia, cooperate to control movement planning and execution?
- How do local and long-range recurrent connections affect information flow in motor circuits?

FURTHER READING

Reviews

Ferreira-Pinto MJ, Ruder L, Capelli P, & Arber S (2018). Connecting circuits for supraspinal control of locomotion. *Neuron* 100:361–374.

Gerfen CR & Surmeier DJ (2011). Modulation of striatal projection systems by dopamine. *Annu Rev Neurosci* 34:441–466.

Ito M (2006). Cerebellar circuitry as a neuronal machine. *Prog Neurobiol* 78:272–303.

Kiehn O (2016). Decoding the organization of spinal circuits that control locomotion. *Nat Rev Neurosci* 17:224–238.

Marder E & Bucher D (2007). Understanding circuit dynamics using the stomatogastric nervous system of lobsters and crabs. *Annu Rev Physiol* 69:291–316.

Shenoy KV, Sahani M, & Churchland MM (2013). Cortical control of arm movements: a dynamical systems perspective. *Annu Rev Neurosci* 36:337–359.

Spinal cord, brainstem, and invertebrates

Bikoff JB, Gabitto MI, Rivard AF, Drobac E, Machado TA, Miri A, Brenner-Morton S, Famojure E, Diaz C, Alvarez FJ, et al. (2016). Spinal inhibitory interneuron diversity delineates variant motor microcircuits. *Cell* 165:207–219.

Esposito MS, Capelli P, & Arber S (2014). Brainstem nucleus MdV mediates skilled forelimb motor tasks. *Nature* 508:351–356.

Graham Brown, T (1911). The intrinsic factors in the act of progression in the mammal. *Proc R Soc Lond B* 84:308–319.

Henneman E, Somjen G, & Carpenter DO (1965). Functional significance of cell size in spinal motoneurons. *J Neurophysiol* 28:560–580.

McLean DL & Fetcho JR (2009). Spinal interneurons differentiate sequentially from those driving the fastest swimming movements in larval zebrafish to those driving the slowest ones. *J Neurosci* 29:13566–13577.

Prinz AA, Bucher D, & Marder E (2004). Similar network activity from disparate circuit parameters. *Nat Neurosci* 7:1345–1352.

Roseberry TK, Lee AM, Lalive AL, Wilbrecht L, Bonci A, & Kreitzer AC (2016). Cell-type-specific control of brainstem locomotor circuits by basal ganglia. *Cell* 164:526–537.

Smith JC, Ellenberger HH, Ballanyi K, Richter DW, & Feldman JL (1991). Pre-Bötzinger complex: a brainstem region that may generate respiratory rhythm in mammals. *Science* 254:726–729.

Stepien AE, Tripodi M, & Arber S (2010). Monosynaptic rabies virus reveals premotor network organization and synaptic specificity of cholinergic partition cells. *Neuron* 68:456–472.

Talpalar AE, Bouvier J, Borgius L, Fortin G, Pierani A, & Kiehn O (2013). Dual-mode operation of neuronal networks involved in left-right alternation. *Nature* 500:85–88.

Yackle K, Schwarz LA, Kam K, Sorokin JM, Huguenard JR, Feldman JL, Luo L, & Krasnow MA (2017). Breathing control center neurons that promote arousal in mice. *Science* 355:1411–1415.

Cortex, cerebellum, and basal ganglia

da Silva JA, Tecuapetla F, Paixao V, & Costa RM (2018). Dopamine neuron activity before action initiation gates and invigorates future movements. *Nature* 554:244–248.

Gallese V, Fadiga L, Fogassi L, & Rizzolatti G (1996). Action recognition in the premotor cortex. *Brain* 119 (Pt 2):593–609.

Gao Z, Davis C, Thomas AM, Economo MN, Abrego AM, Svoboda K, De Zeeuw CI, & Li N (2018). A cortico-cerebellar loop for motor planning. *Nature* 563:113–116.

Georgopoulos AP, Kettner RE, & Schwartz AB (1988). Primate motor cortex and free arm movements to visual targets in three-dimensional space. II. Coding of the direction of movement by a neuronal population. *J Neurosci* 8:2928–2937.

Graziano MS, Taylor CS, & Moore T (2002). Complex movements evoked by microstimulation of precentral cortex. *Neuron* 34:841–851.

Hochberg LR, Bacher D, Jarosiewicz B, Masse NY, Simeral JD, Vogel J, Haddadin S, Liu J, Cash SS, van der Smagt P, et al. (2012). Reach and grasp by people with tetraplegia using a neurally controlled robotic arm. *Nature* 485:372–375.

Hwang EJ, Hauschild M, Wilke M, & Andersen RA (2012). Inactivation of the parietal reach region causes optic ataxia, impairing reaches but not saccades. *Neuron* 76:1021–1029.

Kaufman MT, Churchland MM, Ryu SI, & Shenoy KV (2014). Cortical activity in the null space: permitting preparation without movement. *Nat Neurosci* 17:440–448.

Klaus A, Martins GJ, Paixao VB, Zhou P, Paninski L, & Costa RM (2017). The spatiotemporal organization of the striatum encodes action space. *Neuron* 95:1171–1180.

Markowitz JE, Gillis WF, Beron CC, Neufeld SQ, Robertson K, Bhagat ND, Peterson RE, Peterson E, Hyun M, Linderman SW, et al. (2018). The striatum organizes 3D behavior via moment-to-moment action selection. *Cell* 174:44–58.

Pandarinath C, Nuyujukian P, Blabe CH, Sorice BL, Saab J, Willett FR, Hochberg LR, Shenoy KV, & Henderson JM (2017). High performance communication by people with paralysis using an intracortical brain-computer interface. *Elife* 6:e18554.

Panigrahi B, Martin KA, Li Y, Graves AR, Vollmer A, Olson L, Mensh BD, Karpova AY, & Dudman JT (2015). Dopamine is required for the neural representation and control of movement vigor. *Cell* 162:1418–1430.

Velliste M, Perel S, Spalding MC, Whitford AS, & Schwartz AB (2008). Cortical control of a prosthetic arm for self-feeding. *Nature* 453:1098–1101.

Wagner MJ, Kim TH, Kadmon J, Nguyen ND, Ganguli S, Schnitzer MJ, & Luo L (2019). Shared cortex-cerebellum dynamics in the execution and learning of a motor task. *Cell* 177:669–682.